nature chemistry

SUPPLEMENTARY INFORMATION

DOI: 10.1038/NCHEM.1830

Validation of *N*-myristoyltransferase as an antimalarial drug target using an integrated chemical biology approach

Authors: Megan H. Wright, Barbara Clough, Mark D. Rackham, Kaveri Rangachari, James A. Brannigan, Munira Grainger, David K. Moss, Andrew R. Bottrill, William P. Heal, Malgorzata Broncel, Remigiusz A. Serwa, Declan Brady, David J. Mann, Robin J. Leatherbarrow, Rita Tewari, Anthony J. Wilkinson, Anthony A. Holder, Edward W. Tate.

Supplementary Results

Supplementary figures

Supplementary Tables

Supplementary Figure S1, related to Fig. 1c: Left: electron density map for PvNMT-YnMyr-CoA co-crystal structure (PDB 2YNC). The cofactor YnMyr-CoA is shown in ball-and-stick representation, colored by atom; carbon (gray), oxygen (red), sulfur (yellow), phosphorous (fuchsia) and nitrogen (blue) with associated refined electron density map (2mF_O-dF_C) contoured at a level of 1 σ. **Right:** overlay of YnMyr-CoA in PvNMT (magenta) and Myr-CoA or non-hydrolysable Myr-CoA analogues in PvNMT (green; 4A95), LmNMT (cyan; 2WUU) and ScNMT (yellow; 2P6E), following least-squares superposition of the respective protein backbone atoms in PyMOL (DeLano Scientific).

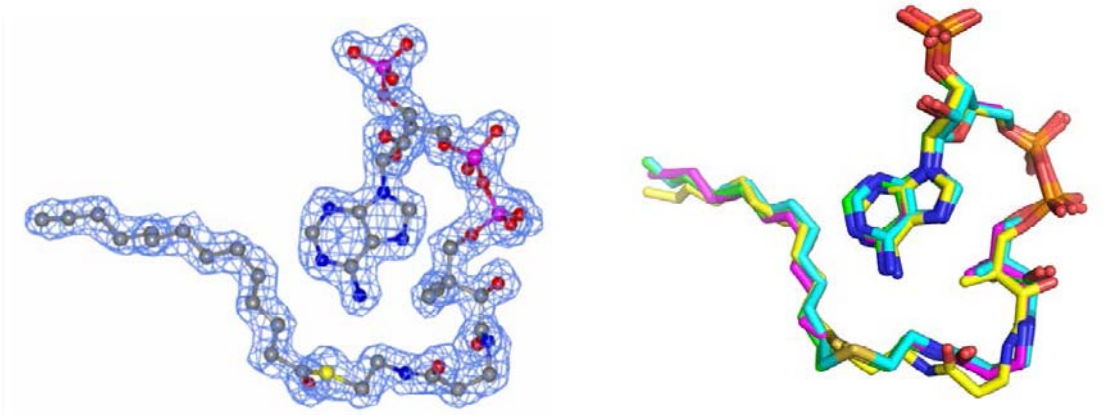

Supplementary Figure S2: representative kinetic data for *Plasmodium vivax* NMT; K_m and V_{max} were determined for a model peptide substrate using a fluorogenic assay, as reported in Goncalves *et al.*[1] (**a**) kinetic data for Myr-CoA; (**b**) kinetic data for YnMyr-CoA.

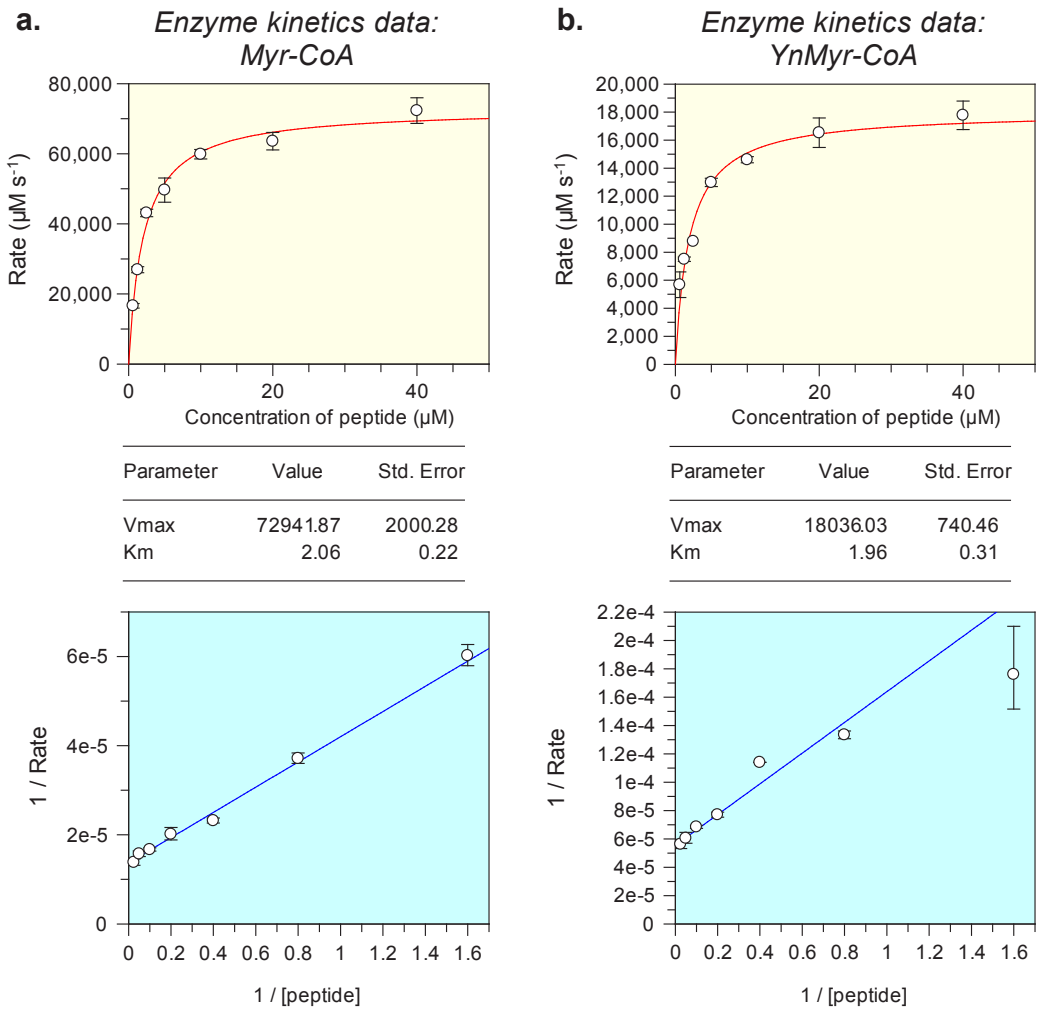

Supplementary Figure S3: Structures of the chemical proteomic reagents used in this study: tagging reagents YnMyr, YnPal, YnMyr-CoA, AHA; capture reagents for CuAAC labeling: AzTB, YnTB, AzKTB.

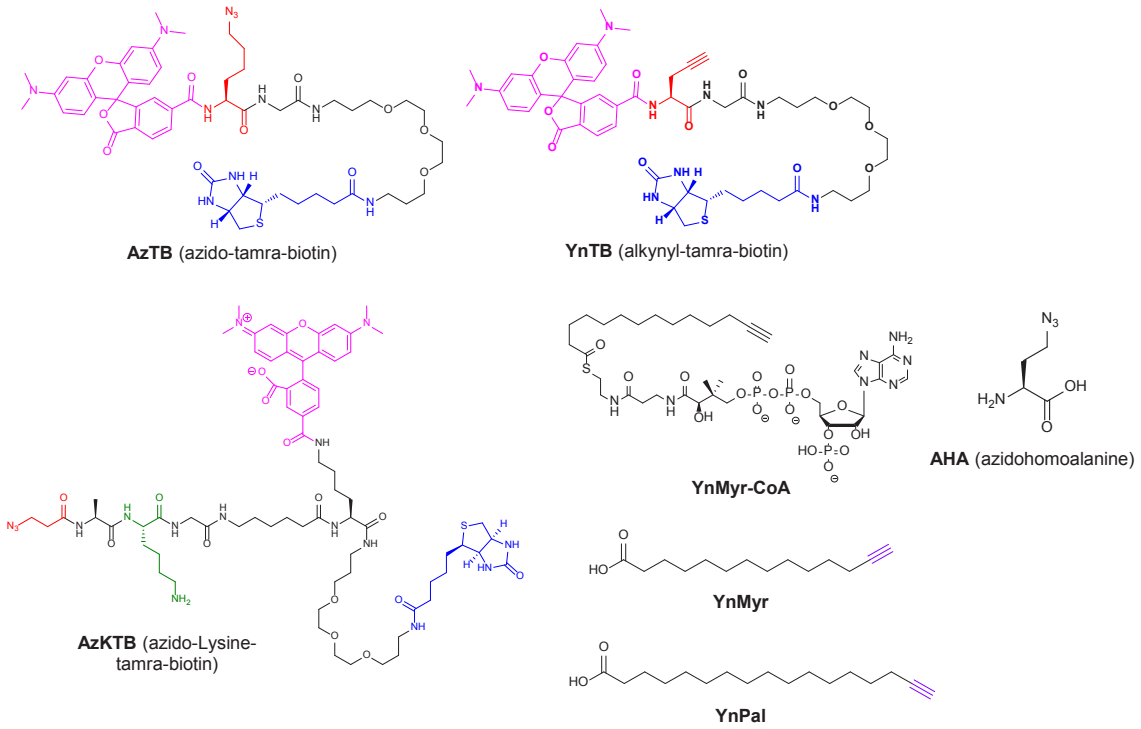

Supplementary Figure S4: YnMyr mimics myristate in blood stage *P. falciparum* cultures. Left: YnMyr concentration series. Middle: Myristic acid added to parasite cultures at increasing concentrations, in combination with 25 μM YnMyr. Right: Parasites treated with 0.1 or 1 μM cycloheximide (CHX, an inhibitor of protein synthesis) and 25 μM YnMyr; a portion of each sample was treated with base (NaOH). Total protein loading by Coomassie blue stain shown in blue.

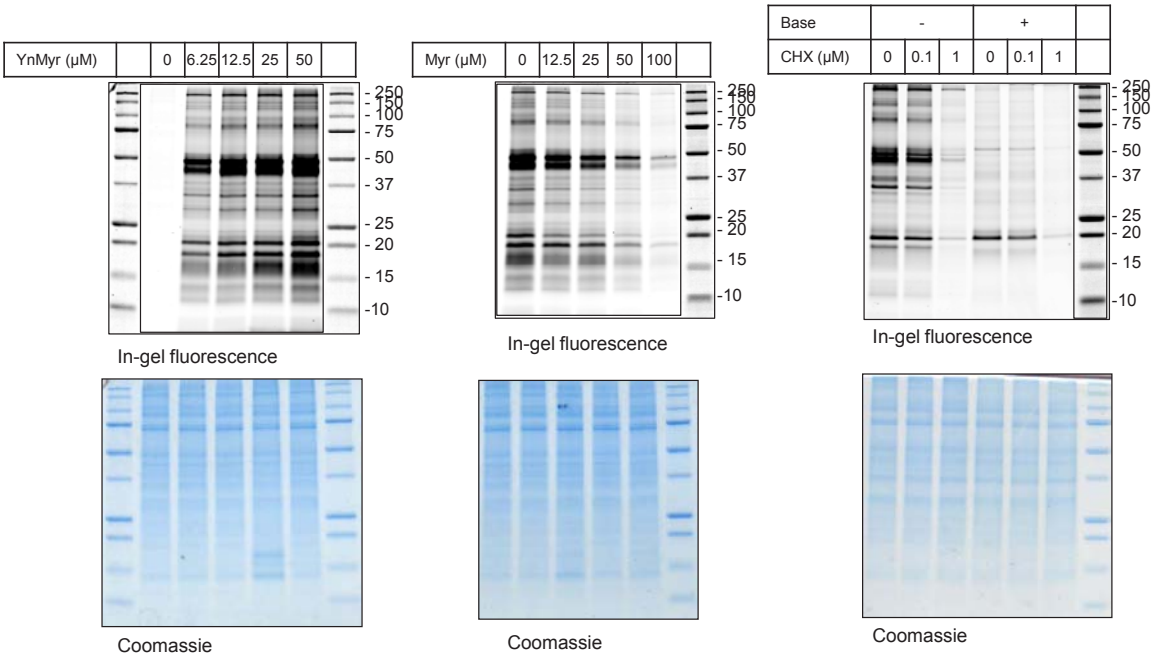

Supplementary Figure S5: Tagged & labeled proteins are efficiently pulled-down on streptavidin-coated beads, and released on elution with SDS. Pull-down of proteins tagged with YnMyr and labeled by CuAAC with AzTB. Left: in-gel fluorescence and Right: Coomassie blue. Lanes 1-2: aliquot taken before pull-down; Lanes 3-4: supernatant after pull-down showing loss of the fluorescently labeled proteins; Lanes 5 and 6: affinity beads boiled to elute modified proteins.

Lane	1	2	3	4	5	6	7
Pull-down	Before		Sup.		Beads		
YnMyr	-	+	-	+	-	+	

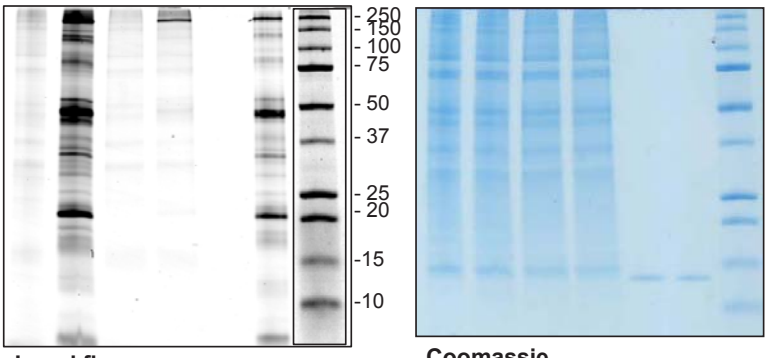

Supplementary Figure S6, related to Fig. 2a: The effect of hydroxylamine or base-treatment on YnMyr tagged proteins. Left: in-gel fluorescence and Coomassie blue of the same gel. Lanes 1-2: untreated samples; Lanes 3-4: samples treated with 1 M hydroxylamine; Lanes 5 and 6: samples treated with 0.2 M NaOH. Right: full images of blots from Figure 2a. Black boxes indicate portion of the blot shown in Fig. 2a. Tagging of *N*-myristoylated proteins CDPK1 and GAP45 is unaffected by hydroxylamine or base treatment, indicative of *N*-acylation. Tagging of GPI-anchored protein MSP1 is affected by base treatment, indicative of *O*-acylation. BiP is shown as a loading control. Four-fold more protein is loaded after pull-down compared to before.

Figure 2a full gels:

Lane	1	2	3	4	5	6
Treatment	-		H		B	
YnMyr	-	+	-	+	-	+

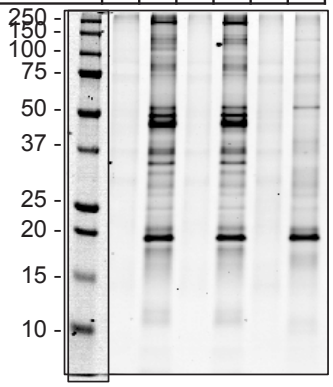

In-gel fluorescence

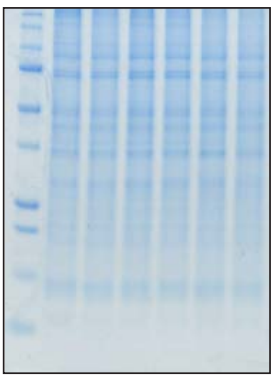

Coomassie

Treatment:
H = hydroxylamine (NH_2OH)
B = base (NaOH)

Figure 2a full blots:

Pull-down	Before						After					
Treatment	-		H		B		-		H		B	
YnMyr	-	+	-	+	-	+	-	+	-	+	-	+

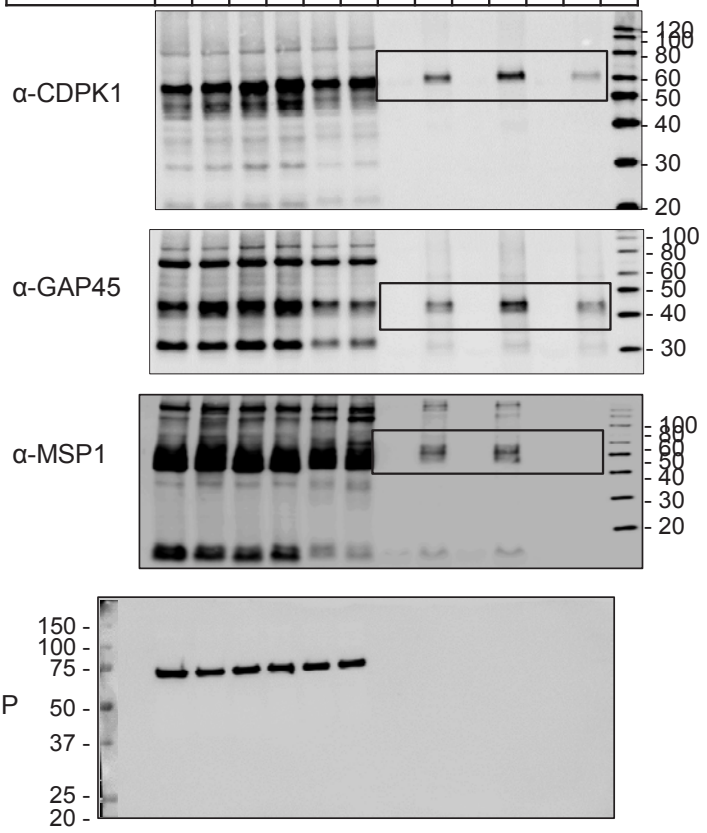

Supplementary Figure S7: *S*-acylation controls. Parasites were tagged with YnPal (left) or YnMyr (right), labeled with AzTB via CuAAC ligation, treated with hydroxylamine (H), or base (B), as indicated, pulled-down onto streptavidin beads and samples analyzed by Western blot. Left: known *S*-palmitoylated protein MTIP is tagged by palmitate analogue YnPal (**Fig. S3**) in a hydroxylamine-dependent manner, indicative of *S*-acylation. Right: YnMyr does not tag MTIP. Molecular weight markers are shown in kDa.

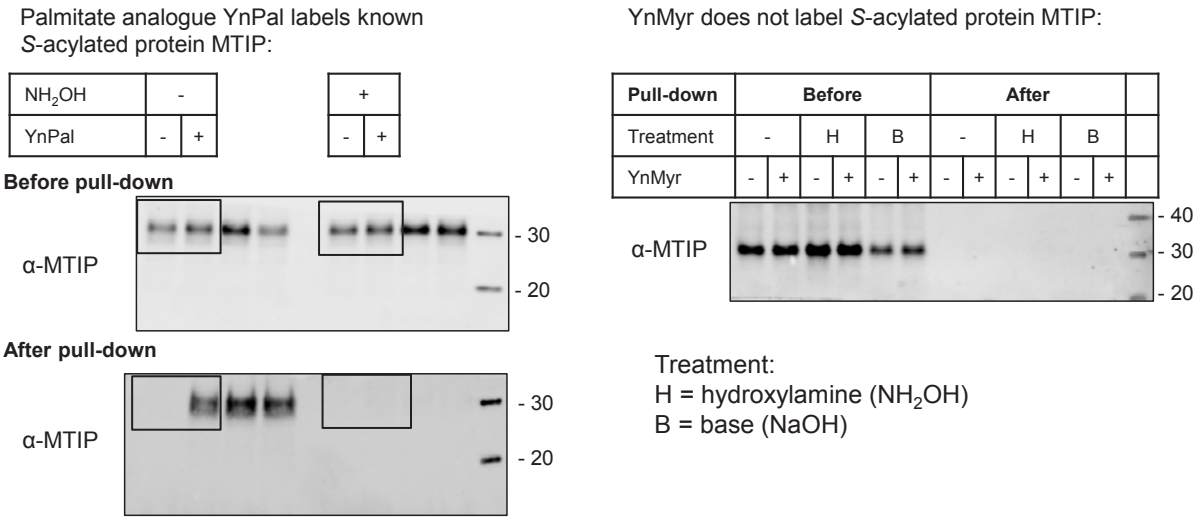

Supplementary Figure S8, related to Fig. 2b: Summary of the N-terminal glycine-containing proteins found by gel-based proteomics. Left: the Coomassie-stained gel sliced into 9 portions during band excision for proteomic identification; including both YnMyr-fed and DMSO-fed control parasites. Right: slices mapped onto a fluorescence gel of YnMyr-tagged sample. Proteins are grouped according to which of the 9 gel slices they were predominantly found in. The dominant proteins in each slice are highlighted in bold.

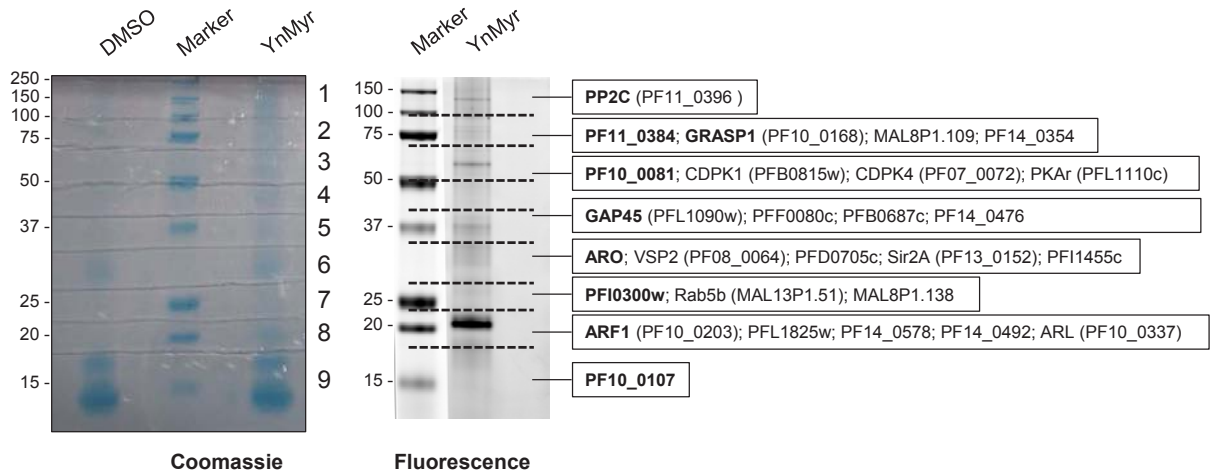

Supplementary Figure S9, related to Table S7: Top: generation of a tagged solution-phase peptide through on-bead tryptic digest using AzKTB. Bottom: example of the MS/MS spectrum resulting from YnMyr tagging of the N-terminus of the 26S proteasome regulatory subunit 4 in live parasites, labeling with AzKTB and enrichment on NeutrAvidin beads, followed by on-bead digestion with trypsin. N-terminal tryptic peptide sequence is *GNTPGGMNNPYGFLGK.

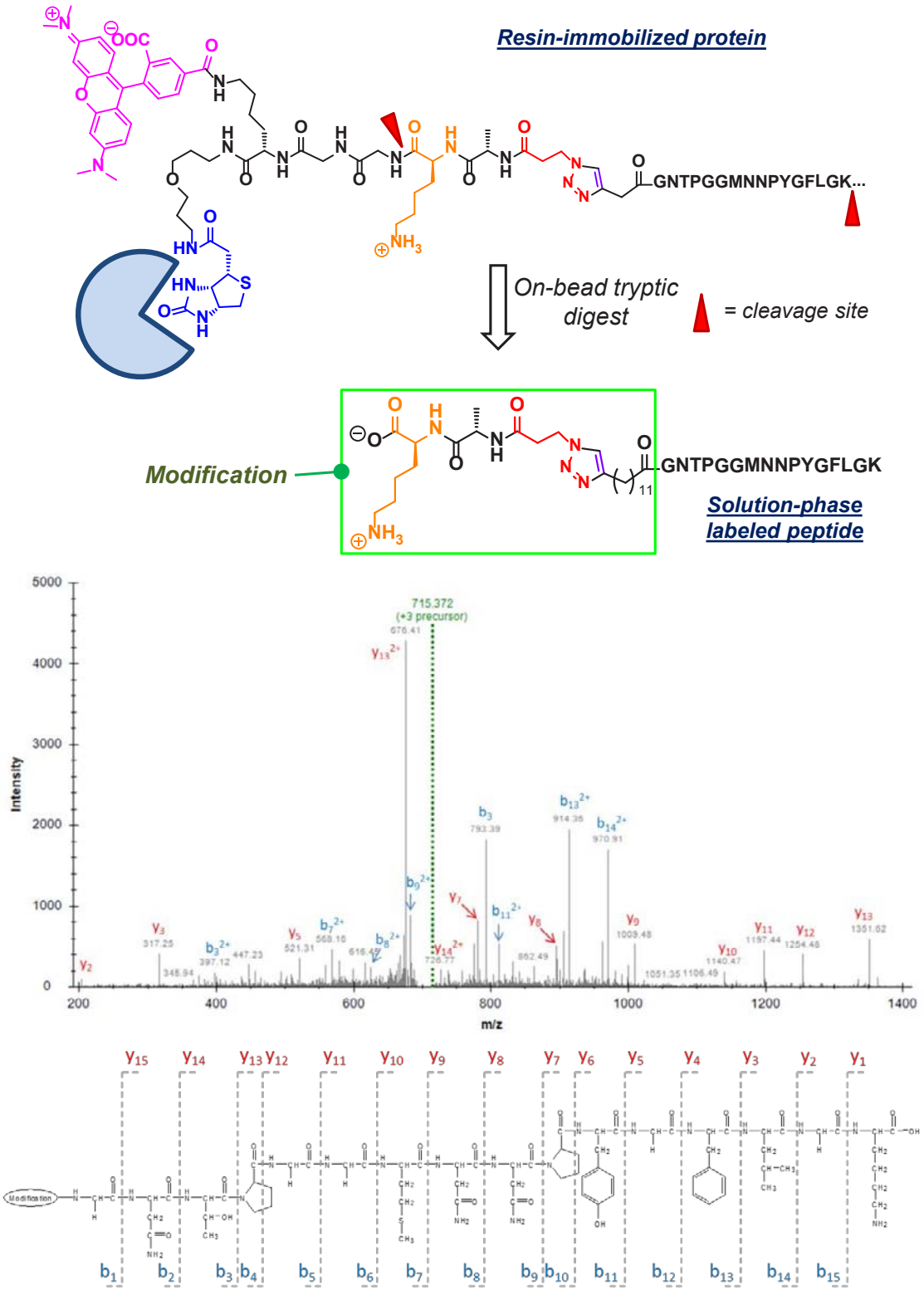

Supplementary Figure S10: Putative or known localization of potential NMT substrates identified (31 proteins containing a base-insensitive modification, an N-terminal glycine and prediction of myristoylation and/or identified modified peptide – see Table S5); from ApiLoc and literature survey.

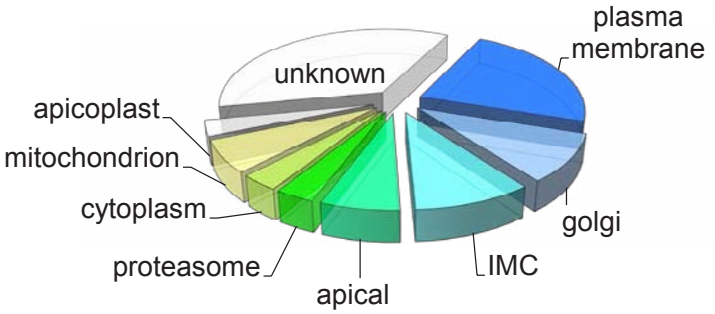

Supplementary Figure S11, related to Figure 4: (**a**) Electron density map of inhibitors **1a** and **2a** in PvNMT. The final, refined electron density map ($2mF_O$-dF_C) contoured at a level of 1 σ are shown in blue. (**b**) Overlay of binding mode of **1a** (left-hand ligand) in PvNMT (magenta) and a series of previously-reported crystal structures for **1a** in LmNMT (PDB: 2WSA; green) or *Homo sapiens* (Hs) NMT (PDB: 3IWE; cyan), following alignment of the protein backbone; right-hand ligand is Myr-CoA or NHM. Images made using PyMOL (DeLano Scientific).

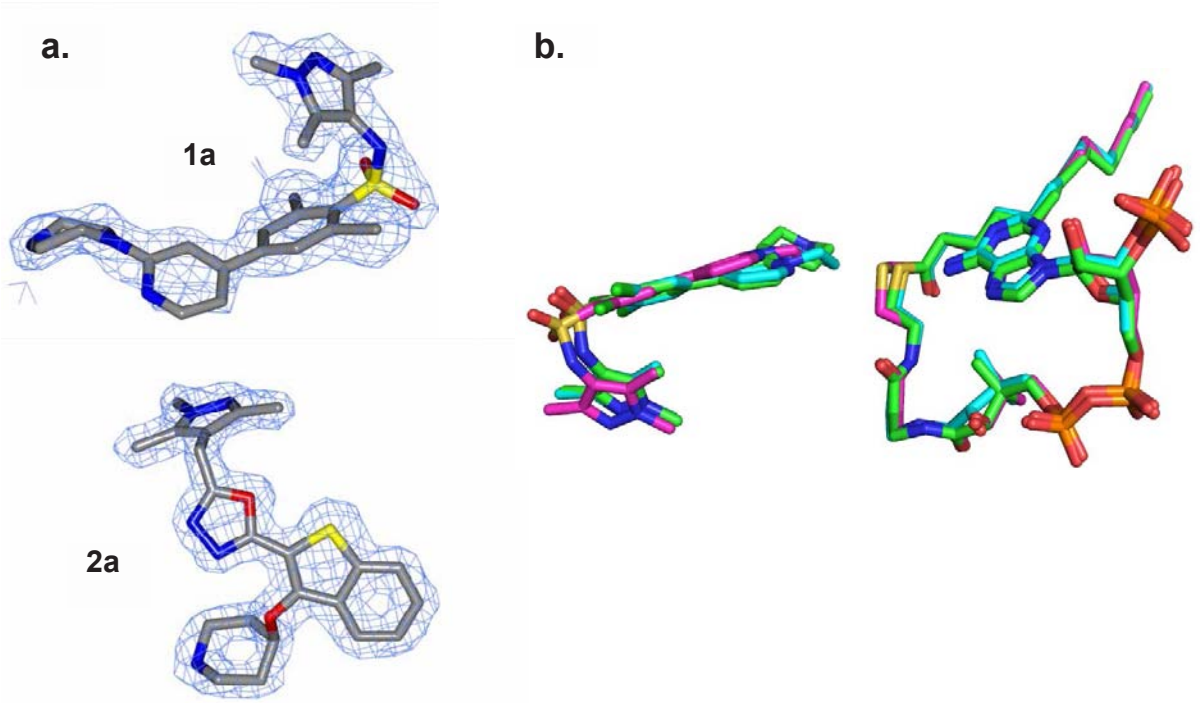

Supplementary Figure S12: Synchronized ring stage parasites at 2h post-invasion were treated with DMSO or **1a** continuously for 96h and Giemsa stained smears prepared at 96h. No parasites were visible in the **1a** treated sample and RBCs remained morphologically normal.

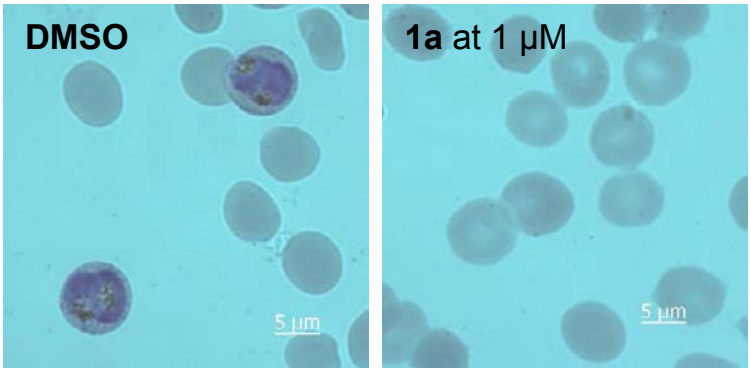

Supplementary Figure S13, related to Figure 5: example of typical changes in in-gel fluorescence prior to base treatment, in response to increasing amounts of inhibitor **1a**. In-gel fluorescence (left) and Coomassie (right) of YnMyr tagged proteins in the presence of **1a**. Samples have not been base-treated to hydrolyze YnMyr attached *via* an ester linkage (i.e. in the GPI-anchor).

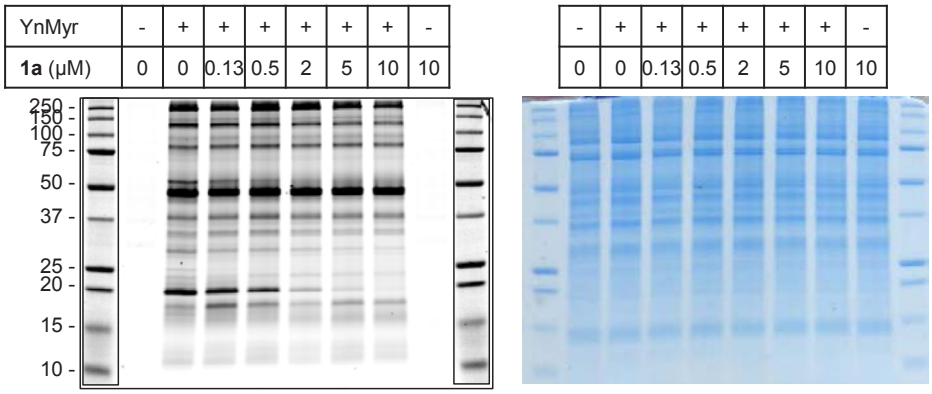

Supplementary Figure S14: in-gel fluorescence provides a linear response for YnMyr tagging. **(a)** In-gel fluorescence (top) and Coomassie (bottom) of a gel loaded with decreasing ratio of YnMyr-tagged lysate, made up to 10 μg total protein with control (DMSO-fed) lysate. **(b)** Plot of the fluorescent signal (quantified across the whole of each lane) relative to proportion of YnMyr lysate.

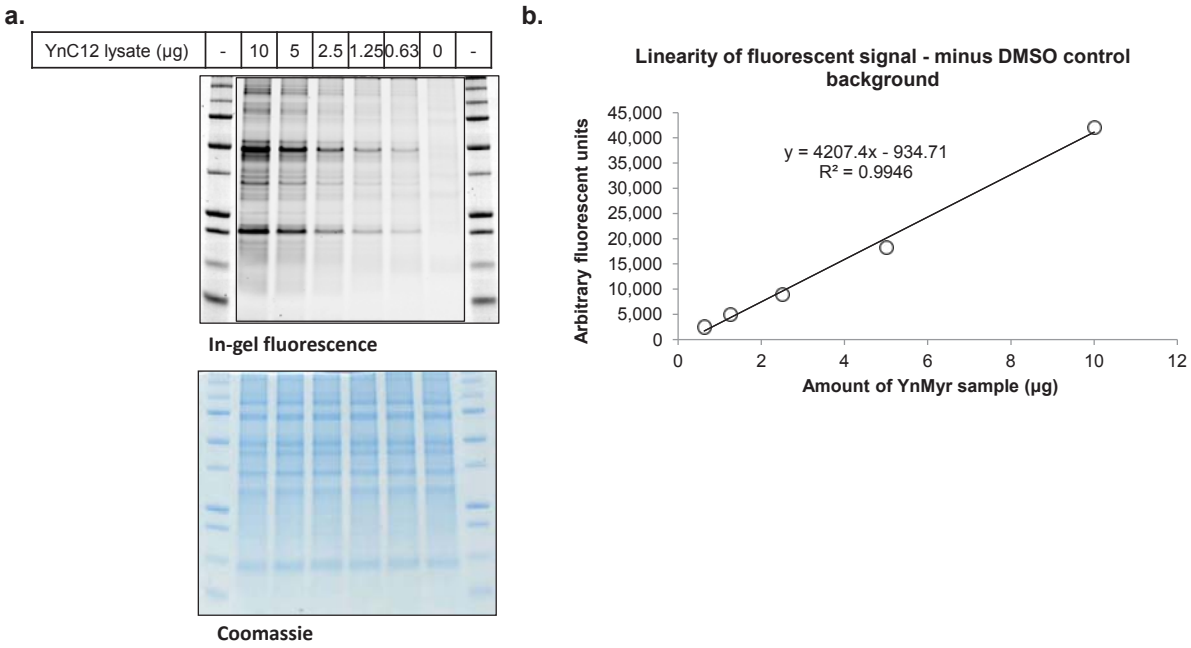

Supplementary Figure S15: AHA (azidohomoalanine) tags newly synthesized proteins in *P. falciparum* and inhibitor **1a** does not affect protein synthesis. **(a)** In-gel fluorescence (top) and Coomassie (bottom) of samples from parasites tagged with increasing amounts of AHA; samples were processed as before but labeled with alkynyl reagent YnTB.[2] **(b)** In-gel fluorescence (top) and Coomassie (bottom) of samples from parasites tagged with AHA in the presence of increasing amounts of protein synthesis inhibitor cycloheximide (CHX). **(c)** In-gel fluorescence (top) and Coomassie (bottom) of samples from parasites tagged with AHA in the presence of NMT inhibitor **1a** or DMSO vehicle. *De novo* protein synthesis in parasites is unaffected by the presence of 10 μM **1a**.

a.

Lane	1	2	3	4	5	6
AHA (μM)	0	6.3	12.5	25	50	-
CHX (μM)	-	-	-	-	-	-

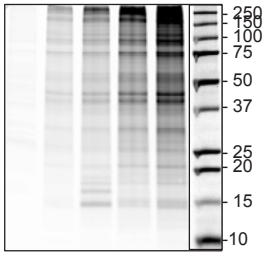

In-gel fluorescence

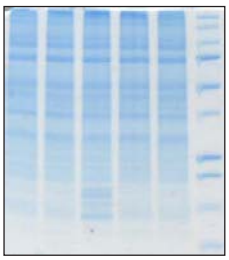

Coomassie

b.

Lane	1	2	3	4
AHA (μM)	-	50	50	50
CHX (μM)	-	0	0.1	1

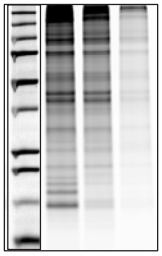

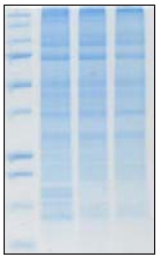

c.

Inhibitor (μM)	0	10	-

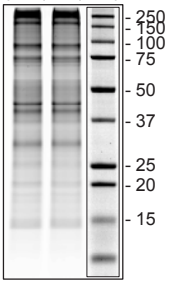

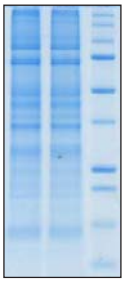

Supplementary Figure S16, related to Figure 2c and Figure 5: YnMyr tagging of ARF and ARO, previously identified by *de novo* proteomics (see Supplementary Table S5), is detectable with antibodies. Left: both proteins exhibit a molecular weight shift upon ligation of AzTB to the YnMyr modification; the tagged & labeled upper band is selectively enriched by pull-down with biotin. Right: modified ARF overlays with the strong fluorescent band at 20 kDa. Lanes 1 & 9 are molecular weight markers in kDa.

Western blot evidence that ARF and ARO detected by proteomics are tagged by YnMyr:

Lane	1	3	4	5	6	7	8	9
Pull-down		Before		Beads		Supnt.		
YnMyr		-	+	-	+	-	+	

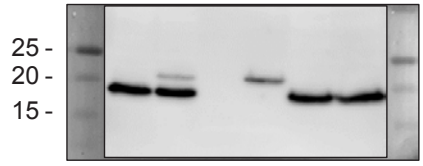

α-ARF; expected MW 20.9 kDa

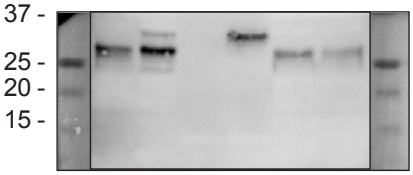

α-ARO (PFD0720w); expected MW 30.8

Tagged ARF overlays with the strong fluorescent band at 20 kDa:

Lane	1	3	4	5	6	7	8	9
Pull-down		Before		Beads		Supnt.		
YnMyr		-	+	-	+	-	+	

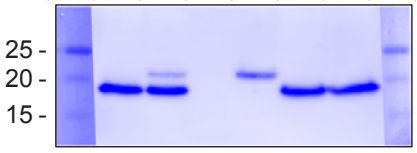

α-ARF WB

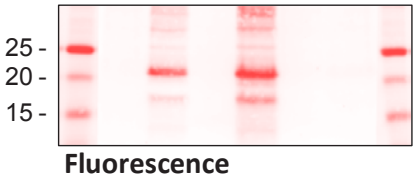

Fluorescence

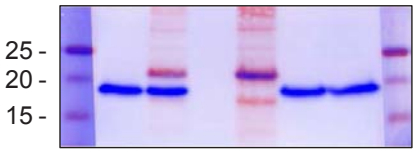

Overlay

Supplementary Figure S17, related to Figure 5: inhibitor **1a** affects YnMyr tagging of CDPK1, GAP45, ARF and ARO but has no impact on tagging of GPI-anchored protein MSP1. Western blots showing samples before and after pull-down. Four- to five-fold more sample was loaded 'after' pull-down compared to lanes marked 'before', as indicated. BiP is a housekeeper protein used to control for loading.

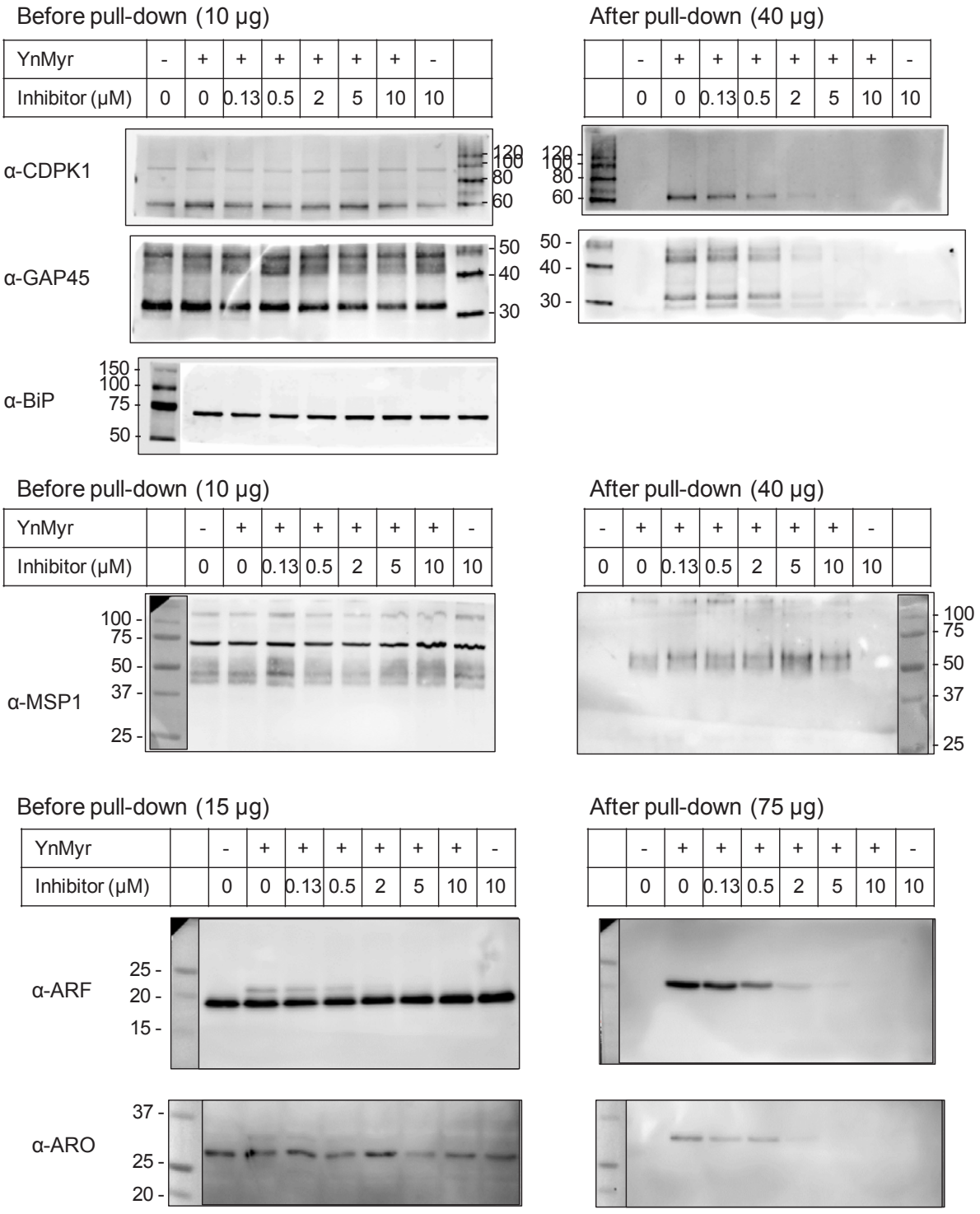

Supplementary Figure S18, related to Figure 5: Quantifying the response of tagged *N*-myristoylated proteins to NMT inhibition with compound **1a**. Left: gel shown in Figure 4b. Fluorescence intensity of bands 1 to 3 was plotted (graph, right) and GraFit (Erithacus Software, UK) used to calculate the half maximal inhibitory concentration for in-cell inhibition (TC_{50}, table). Western blots (WB) for CDPK1, GAP45 and ARF (Fig. S15) were also quantified and are shown on the graph. Band 1 consists predominantly of ARF1, as shown in proteomic analysis (see Fig. S8) and by Western blot (see Fig. S15).

Figure 4b, gel data:

YnMyr	-	+	+	+	+	+	+	-
Inhibitor (µM)	0	0	0.13	0.5	2	5	10	10

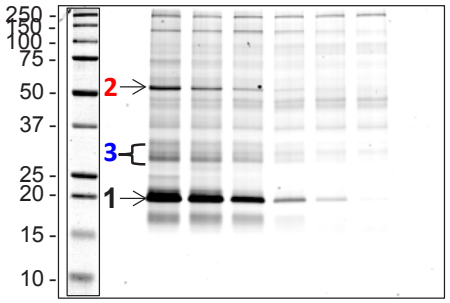

In-gel fluorescence

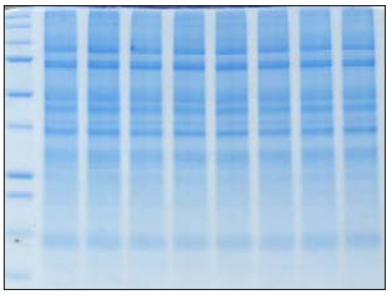

Coomassie

Calculation of TC_{50} for inhibitor 1a:

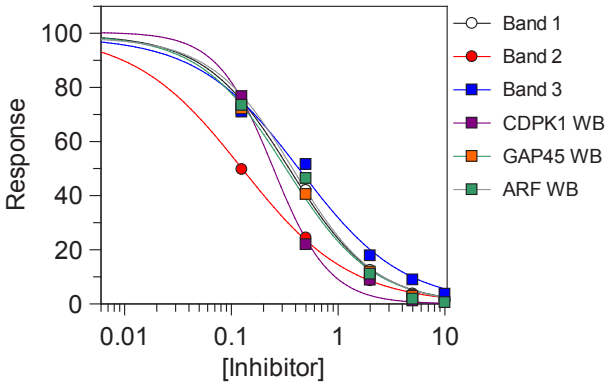

	In-cell TC_{50} (nM)	Slope factor
Band 1	346 ±16	1.09 ±0.05
Band 2	126 ±5	0.86 ±0.03
Band 3	427 ±49	0.89 ±0.08
CDPK1	247 ±31	1.65 ±0.24
GAP45	327 ±28	1.07 ±0.08
ARF	371 ±38	1.11 ±0.11

Supplementary Figure S19, related to Figure 5: Measuring inhibition of NMT by a panel of five compounds. In-gel fluorescence (top) after base-treatment of the gel to remove GPI-anchor tagging, Coomassie blue (bottom) of samples from parasites tagged with YnMyr in the presence of five inhibitors as indicated. ARF1 band, used for quantification, is indicated by a black arrow.

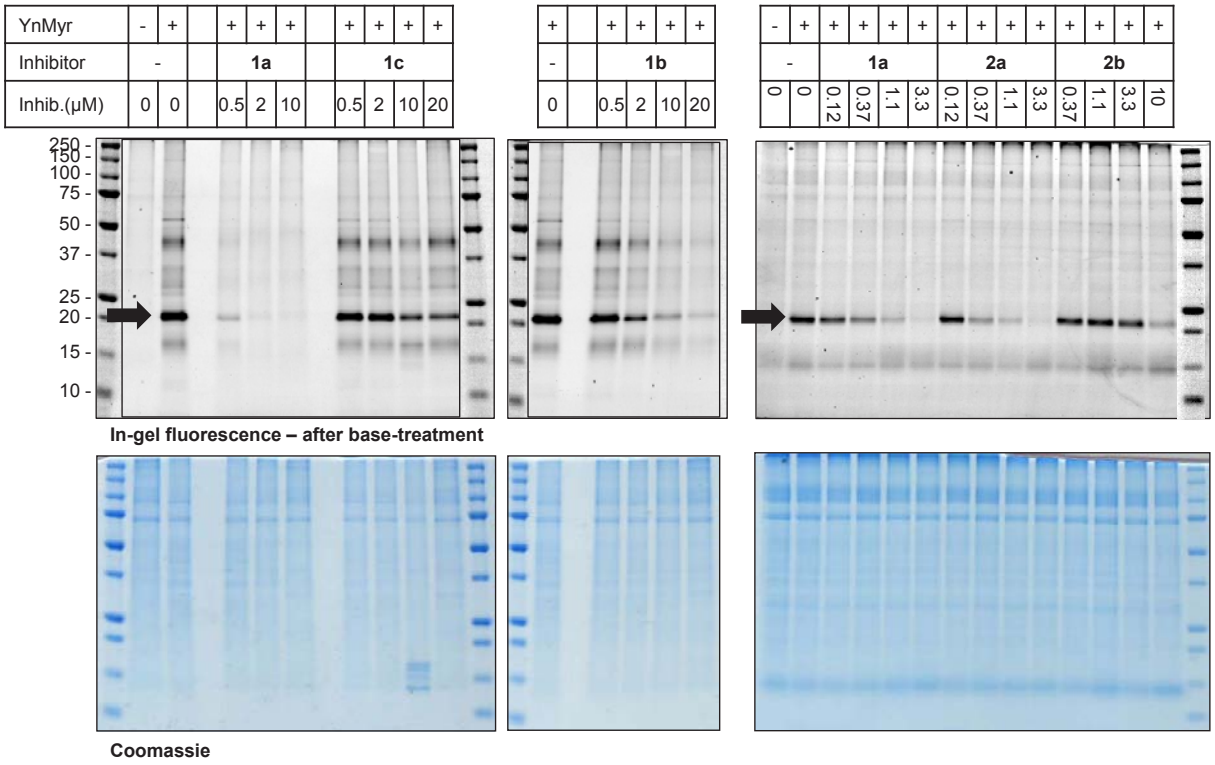

Supplementary Figure S20, related to Figure 5: Measuring TC_{50} for NMT across series **1** and **2** by in-gel fluorescence quantification of ARF1 band at ~20kDa. TC_{50} curves for *P. falciparum* inhibitors plotted in GraFit (Erithacus Software, UK). Technical replicates: *black* curve is best fit, *green* curve is back-corrected fit (background corrected to zero), *red* curve is fully corrected (zero to 100 % response).

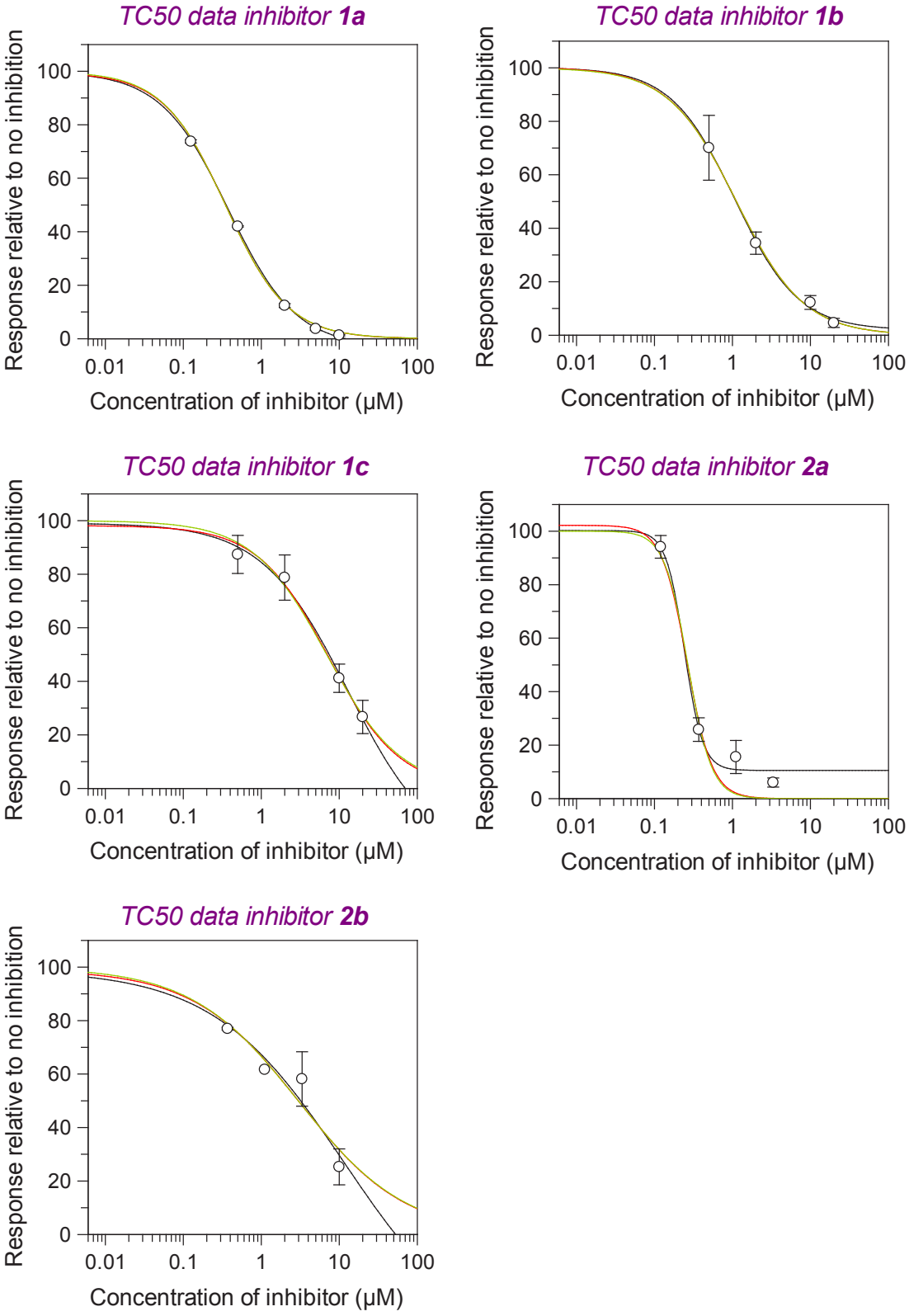

Supplementary Figure S21, related to Figure 6: Synchronized young ring stage parasites (~2h PI) were treated with DMSO or 1 μM **1a** and thin smears prepared at 45h PI; left: parasites were visualized under Giemsa or DAPI stain, showing altered numbers of nuclei (DAPI image shows one representative iRBC, scale bar = 5 μm); right: nuclei counted in 50 iRBCs, +/- inhibitor; uninfected RBCs were morphologically normal.

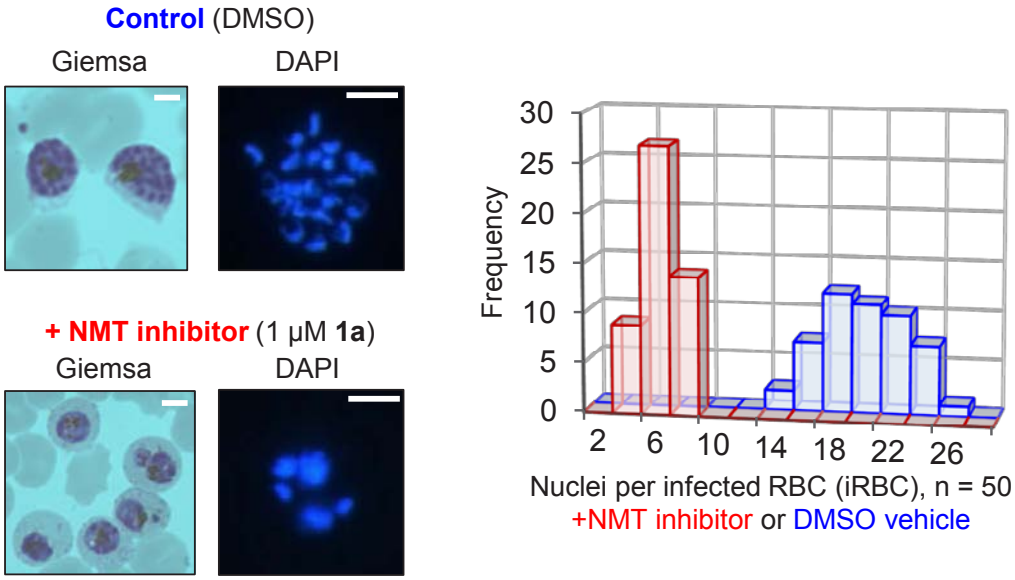

Supplementary Figure S22, related to Figure 6: Synchronized young ring stage parasites (~2h PI) were treated with DMSO or 1 μM **1a**, and Giemsa stained thin smears were prepared at the time points indicated. 1000 RBCs were counted at each time point and % infected RBCs (iRBCs) determined.

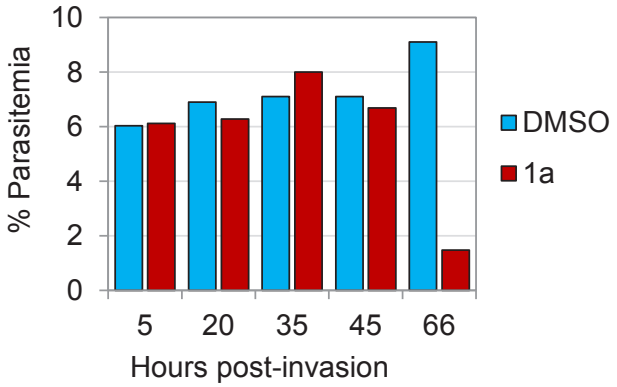

Supplementary Table S1: Prediction of *N*-myristoylation by bioinformatic tools.

See attached Excel spreadsheet.

All *P. falciparum* proteins containing an N-terminal MG motif were retrieved from PlasmoDB. Each protein N-terminal sequence was submitted to two online *N*-myristoylation predictive tools, the Myristoylator (Myrist.) and the MYR Predictor (MYR). In columns H & J proteins are assigned as M = predicted to be *N*-myristoylated, or NM = not *N*-myristoylated; scores are also given. Columns I & K give the shorthand for columns H & J: ++ = strong prediction; + = medium prediction; - = weak/not predicted.

Table S2: X-ray data collection and refinement statistics.

PDB accession code	PvNMT-YnMyrCoA **2YNC**	PvNMT-NHM-**1a** **2YND**	PvNMT-NHM-**2a** **2YNE**
Cell dimensions *a*, *b*, *c*	57.37, 118.74, 176.73	57.45, 119.05, 176.73	57.62, 121.85, 179.16
Space Group	$P2_12_12_1$	$P2_12_12_1$	$P2_12_12_1$
Data collection			
Beamline / Wavelength	DLS i04 / 0.9795	DLS i04-1 / 0.9173	DLS i04-1 / 0.9200
Detector type	ADSC Q315r CCD	CMOS Pilatus 2M	CMOS Pilatus 2M
Images x oscillation (°)	720 x 0.25	900 x 0.2	900 x 0.2
Resolution (Å)	119–1.75 (1.84–1.75)	60–1.89 (1.99–1.89)	45–1.72 (1.81–1.72)
R_{sym} (%) [b]	16.6 (73.4)	17.0 (64.3)	16.0 (70.8)
$I/\sigma I$	9.0 (2.7)	8.4 (2.7)	7.8 (2.5)
Completeness (%)	98.8 (97.9)	99.7 (99.5)	99.6 (99.8)
Redundancy	7.4 (7.5)	6.6 (6.4)	6.5 (6.7)
Refinement			
No. unique reflections	119985	97896	134040
R_{work} / R_{free} [c]	15.9 / 20.3	16.8 / 22.3	17.3 / 21.8
No. atoms	11267	11146	11389
Protein	9790	9567	9708
Ligand	n/a	96	90
Co-factor	189	192	192
Water	1263	1268	1375
B-factors (Å^2)			
All atoms	13.5	17.2	17.8
Protein	12.6	16.2	16.6
Ligand	n/a	33.3	13.9
Co-factor	10.1	12.7	12.7
Water	22.4	24.7	26.3
R.m.s.deviations [d]			
Bond lengths (Å)	0.021	0.021	0.024
Bond angles (°)	2.114	2.133	2.280

[a]Highest resolution shell is shown in parentheses.

[b]$R_{sym} = \Sigma_h\Sigma_l |I_{hl} - \langle I_h \rangle| / \Sigma_h\Sigma_l\langle I_h \rangle$, where I_l is the l^{th} observation of reflection h and $\langle I_h \rangle$ is the weighted average intensity for all observations *l* of reflection h.

[c] $R_{work} = \sum||F_o| - |F_c||/\sum|F_o|$ where F_o and F_c are the observed and calculated structure factor amplitudes, respectively. R_{free} is the R_{cryst} calculated with 5% of the reflections omitted from refinement.

[d] Root-mean-square deviation of bond lengths or bond angles from ideal geometry.

Supplementary Table S3, related to Fig. 3: Total proteomic data.

See attached Excel spreadsheet.

Total proteomic data for four separate chemical proteomic experiments. No base: gel-free proteomic identification; samples were not treated with base prior to enrichment. Base 1: gel-free; samples were treated with base prior to enrichment. Base 2: replicate of Base 1. Base GEL: gel-based proteomic identification; samples were treated with base prior to enrichment. For each experiment, DMSO controls were processed in parallel with YnMyr samples. Only high-confidence identifications (>99 %) are shown. Non-specific proteins, defined as those where fold-enrichment YnMyr/DMSO was <4 in 2 or more experiments, have been removed. Number of assigned spectra, unique peptides and % sequence coverage is given for each sample.

Supplementary Table S4, related to Fig. 3: Base-sensitive hits. Listed proteins are those that are identified with >99 % confidence (0.0 % false-discovery rate for both peptide and protein identification) and enriched in a base-sensitive manner. Prediction and/or identification in a recent proteomic study of GPI-anchored proteins by Gilson *et al*. is given in the final column.[3]

Protein name	PlasmoDB ID	MW	No base			Identified in Gilson *et al.*
			Assigned spectra		% coverage	
			DMSO	YnMyr	YnMyr	
Potential GPI-anchored proteins						
Merozoite surface protein 1	PFI1475w	196 kDa	29	360	54%	yes
Cysteine-rich surface protein, Pf92	PF13_0338	93 kDa	0	65	40%	yes
Merozoite surface antigen 2, MSP2	PFB0300c	28 kDa	0	54	42%	yes
6-cysteine protein, Pf38	PFE0395c	41 kDa	0	27	37%	yes
Surface protein, Pf113	PF14_0201	113 kDa	0	24	24%	predicted
Rifin-like protein, RAMA	MAL7P1.208	104 kDa	0	16	18%	yes
6-cysteine protein, Pf12	PFF0615c	39 kDa	0	15	36%	yes
Uncharacterized protein	PFF0335c	35 kDa	0	14	33%	yes/not pred.
GPI-anchored micronemal antigen, GAMA	PF08_0008	85 kDa	0	11	12%	predicted
Apical merozoite protein, Pf34	PFD0955w	39 kDa	0	10	23%	yes
Apical sushi protein, ASP	PFD0295c	85 kDa	0	7	14%	yes
Merozoite surface protein 10, MSP10	PFF0995c	61 kDa	0	6	13%	yes
Conserved Plasmodium protein	PF11_0373	77 kDa	0	5	7%	predicted
Merozoite surface protein 5, MSP5	PFB0305c-b	30 kDa	0	3	12%	yes
Merozoite surface protein 4, MSP4	PFB0310c	31 kDa	0	2	15%	yes
Other base-sensitive proteins						
Bifunctional dihydrofolate reductase-thymidylate synthase	PFD0805w	72 kDa	0	6	10%	no
Organic anion transporter	PFF0690c	97 kDa	0	6	5%	no
Uncharacterized protein	MAL8P1.62	32 kDa	0	3	13%	no
Uncharacterized protein	PF08_0035	138 kDa	0	3	2%	no
Folate/biopterin transporter, putative	PF11_0172	51 kDa	0	2	6%	no
Importin beta, putative	PF08_0069	100 kDa	0	2	2%	no

DOI: 10.1038/NCHEM.1830

Supplementary Table S5, related to Fig. 3: Base-insensitive proteins. All proteins were identified with >99 % confidence, 0.0 % false-discovery rate for both peptide and protein identification. No proteins were found in any DMSO control at >1 high confidence spectral count. Listed proteins are those identified in the gel-free base-insensitive sample set; the number of assigned spectra is listed per protein for standard sample handling ('non-base') and following base treatment of the lysate ('base'). Prediction of *N*-myristoylation was by two online bioinformatic tools (the MYR predictor and the Myristoylator): ++ = strong prediction; + = medium prediction; - = weak/not predicted. † = internal *N*-myristoylation motif (MLFFFFFVHN**M**GNTVNKK). Those proteins also identified in the gel-based analysis (Table S6) and in the AzKTB experiment (Table S7) where the modified *N*-acylated peptide was identified are indicated. * = N-terminal modified peptide not unique to protein; # = only one peptide identified for this protein. MS evidence in blood stages retrieved from PlasmoDB (10/12/12): Y = evidence; L = limited evidence (<1 spectral count per study); N = no previous evidence.

Protein name	PlasmoDB ID	Previous MS evidence in RBC stages	^MG	Prediction		Modified peptide	Assigned spectra				% Coverage
				MYR	Myrist.		No base	Base 1	Base 2	Base Gel	Base 1
N-terminal residue is glycine											
ADP-ribosylation factor 1	PF10_0203	Y	Y	-	++	Y*	71	129	157	277	85%
26S proteasome regulatory subunit 4	PF10_0081	Y	Y	-	-	Y	51	99	92	199	64%
Protein phosphatase 2C	PF11_0396	Y	Y	++	++	Y	41	58	46	130	31%
Calcium-dependent protein kinase 1	PFB0815w	Y	Y	++	++	Y	16	33	27	48	44%
Golgi re-assembly stacking protein 1	PF10_0168	Y	Y	++	-	Y	15	18	12	27	25%
Uncharacterized protein	PF14_0578	Y	Y	++	-	Y	14	24	21	33	47%
Conserved Plasmodium membrane protein	PF11_0384	L	Y	++	+		14	18	15	28	16%
Glideosome-associated protein 45	PFL1090w	Y	Y	++	++		13	28	31	73	30%
Conserved Plasmodium membrane protein	PFL1825w	Y	Y	++	++	Y	12	18	12	58	29%
Armadillo repeats only protein (ARO)	PFD0720w	Y	Y	++	+	Y	10	21	15	53	42%
Developmental protein	PFI0300w	Y	Y	++	++		9	17	16	35	51%
Protein phosphatase 2b regulatory subunit	PF14_0492	Y	Y	++	-	Y	9	22	9	10	55%
Calcium-dependent protein kinase 4	PF07_0072	Y	Y	++	++	Y	8	18	12	18	28%
TPR-like domain containing protein	PFF0080c	L	Y	+	++	Y* #	6	11	7	16	47%
Uncharacterized protein	PFD0705c	L	Y	-	-		6	7	5	15	14%
ADP-ribosylation factor-like protein	PF10_0337	Y	Y	+	++	Y	5	6	8	12	25%

BSD domain	PFD1095w	N	Y	-	++		5	6	3		32%
Rab5b, GTPase	MAL13P1.51	N	Y	++	-		4	9	5	15	36%
Transcriptional regulatory protein sir2 homologue	PF13_0152	N	Y	-	-		3	9	8	10	23%
Vacuolar protein-sorting protein, VPS2	PF08_0064	Y	Y	++	++		3	7	6	24	22%
Protein phosphatase	MAL8P1.109	Y	Y	+	++	Y #	3	5	6	13	9%
Conserved protein	PF10_0107	L	Y	++	++	Y	3	6	7	4	28%
RING zinc finger protein	PFB0687c	L	Y	-	++		2	2	2	11	5%
Cytochrome C oxidase copper chaperone	PF10_0252	L	Y	-	++		2	5			37%
Serine/threonine protein kinase	PF14_0476	Y	Y	++	++	Y #		3	5	5	8%
Alpha/beta hydrolase	MAL8P1.138	N	Y	-	++	Y #		3	4	5	12%
Uncharacterized protein	PFI1455c	N	Y	++	++			3	3	2	10%
ADP-ribosylation factor-like protein	PFI1005w	L	Y	++	++	Y		3	3		10%
CAMP-dependent protein kinase regulatory subunit	PFL1110c	Y	Y	++	+			2		3	5%
Mitochondrial import receptor subunit, TOM22	PFE1230c	L	Y	+	++		2		3		N/A
Uncharacterized protein	PFI0675w	N	Y	++	++				3		N/A
Uncharacterized protein	PFD0185c	Y	Y	-	++			4			7%
Pantothenate kinase	PF14_0354	Y	Y	-	+					10	N/A
N-terminal residue other than glycine											
Proteasome 26S regulatory subunit	PFB0260w	Y					10	12	3	31	15%
26S proteasome regulatory subunit 7	PF13_0063	Y					6	12	7	34	36%
Merozoite Surface Protein 7, MSP7	PF13_0197	Y					3	7	3	4	13%
Eukaryotic initiation factor 5a	PFL0210c	Y					2	3			27%
Spermidine synthase	PF11_0301	Y					2	2			6%
ADP-ribosylation factor	MAL13P1.297	N	N†	+	++		2	2			10%
26S proteasome regulatory subunit	PF13_0033	Y					2			19	N/A
Signal peptide peptidase	PF14_0543	Y							2	2	N/A
Tat-binding protein homolog	PFL2345c	Y						2		10	9%
60S ribosomal protein L40/UBI	PF13_0346	Y						3		4	12%
HAP protein	PF14_0078	Y						2		3	5%

DOI: 10.1038/NCHEM.1830

Supplementary Table S6, related to Fig. 2b and S8: Gel-based analysis. Counts (total) indicates the number of assigned spectra for that protein found in all gel slice samples combined; Counts (slice) indicates the number of assigned spectra in the indicated slice.

Gel slice	Protein name	Uniprot ID	Molecular weight	PlasmoDB ID	Counts (total)	Counts (slice)
1	Protein phosphatase 2C, PP2C	Q8IHY0	105 kDa	PF11_0396	130	42
2	Cleft lip and palate associated transmembrane protein-related	Q8IHZ2	82 kDa	PF11_0384	28	14
	Golgi re-assembly stacking protein 1, GRASP1	C6S3C8	67 kDa	PF10_0168-b	27	17
	Protein phosphatase, putative	C0H4T6	64 kDa	MAL8P1.109	13	8
	Pantothenate kinase, putative	Q8IL92	91 kDa	PF14_0354	10	7
3	26S proteasome regulatory subunit 4, putative	Q8IJW0	50 kDa	PF10_0081	199	82
	Calcium-dependent protein kinase 1, CDPK1	P62344	61 kDa	PFB0815w	48	33
	Calcium-dependent protein kinase 4, CDPK4	Q8IBS5	61 kDa	PF07_0072	18	18
	CAMP-dependent protein kinase regulatory subunit, PKAr	Q7KQK0	51 kDa	PFL1110c	3	3
5	Glideosome-associated protein 45, GAP45	Q8I5I8	24 kDa	PFL1090w	73	29
	RING zinc finger protein, putative	Q8I660	34 kDa	PFB0687c	11	7
	Serine/threonine protein kinase, putative	Q8IKX5	44 kDa	PF14_0476	5	3
5+6	TPR-like domain containing protein	C6KSL8	34 kDa	PFF0080c	16	8
6	Armadillo repeats only protein, ARO	C0H4A5	31 kDa	PFD0720w	53	24
	Vacuolar protein-sorting protein, VPS2	Q8IAZ9	25 kDa	PF08_0064	24	16
	Putative uncharacterized protein	Q8I1U2	27 kDa	PFD0705c	15	12
	Transcriptional regulatory protein sir2 homologue, Sir2A	Q8IE47	30 kDa	PF13_0152	10	9
	Putative uncharacterized protein	Q8I2L4	32 kDa	PFI1455c	2	2
7	Developmental protein, putative	Q8I388	22 kDa	PFI0300w	35	23
	Rab5b, GTPase	Q76NM7	23 kDa	MAL13P1.51	15	10
	Alpha/beta hydrolase, putative	C0H4R4	28 kDa	MAL8P1.138	5	5
8	ADP-ribosylation factor 1, ARF1	Q7KQL3	21 kDa	PF10_0203	277	126
	Conserved Plasmodium membrane protein	Q8I546	24 kDa	PFL1825w	58	27
	Putative uncharacterized protein	Q8IKM6	17 kDa	PF14_0578	33	10
	Protein phosphatase 2b regulatory subunit, putative	Q8IKV9	20 kDa	PF14_0492	10	10
	ADP-ribosylation factor-like protein	Q8IJ63	20 kDa	PF10_0337	12	10
9	Conserved protein	Q8IJT5	17 kDa	PF10_0107	4	4

Supplementary Table S7, related to Fig. 3: modified peptides identified following capture with AzKTB. A search was performed for modification with the AzKTB fragment (addition of 520.34 kDa) on the N-terminus of any protein for YnMyr treated and DMSO treated samples. The minimum peptide length allowed was five amino acids; two missed cleavages were allowed.

Any protein N-terminus; YnMyr					
Sequence	**Uniprot ID**	**PlasmoDB ID**	**Unique Protein**	**Known hit**	**Unique Peptides**
High confidence. 2 or more unique peptides and protein was hit in previous analyses.					
GNTPGGM(Ox)NNPYGFLGK	Q8IJW0	PF10_0081	Y	Y	7
GNTPGGMNNPYGFLGK	Q8IJW0	PF10_0081	Y	Y	7
GAYLSSPK	Q8IHY0	PF11_0396	Y	Y	5
GAGQTK	C6S3C8	PF10_0168	Y	Y	3
GCSQSSNVK	P62344	CPK1	Y	Y	3
GCTVSNLK	Q8I546	PFL1825w	Y	Y	3
GNLCCSNNDIK	Q8IKM6	PF14_0578	Y	Y	3
GLIFSSIFSR	Q8IJ63	PF10_0337	Y	Y	2
GNNCCAGR	C0H4A5	PFD0720w	Y	Y	2
GNTQAILSEK	Q8IKV9	PF14_0492	Y	Y	2
GNTVTTFFR	Q8I2U8	PFI1005w	Y	Y	2
GLYVSR	Q7KQL3; C0H4G8	ARF1; PFE1515w	N	Y N	9 1
Medium confidence. Only 1 unique peptide but protein was hit in previous analyses.					
GAFGSK	C6KSL8; C6KTE5	PFF0080c; PFF1505w	N	Y N	1 1
GNIVSCCSLDENKK	Q8IJT5	PF10_0107	Y	Y	1
GNVLNR	C0H4R4	MAL8P1.138	Y	Y	1
GSTISK	Q8IKX5	PF14_0476	Y	Y	1
GTCISFLK	C0H4T6	MAL8P1.109	Y	Y	1
Low confidence. Only 1 unique peptide and protein not a hit in previous analyses.					
MTFLKLTNRK	Q8IDB6	MAL13P1.289	Y	N	1
Any protein N-terminus; DMSO					
Low confidence. Only 1 unique peptide and protein not a hit in previous analyses.					
ESNIGTEK	Q8I316	PFI0665w	Y	N	1
LSLKNVK	Q8I3Z8	PFE0530w	Y	N	1
MDALILDEQIR	Q8IDA3	MAL13P1.299	Y	N	1
MGNSLSLCLLR	Q8IDT6	PF13_0218	Y	N	1
MKCTSVNIR	Q8I239	PfPIP5K/NCS	Y	N	1
MVDSGCSILIR	Q8II95	PF11_0279	Y	N	1
MYRADIIR	Q8IIH1	PF11_0203	Y	N	1
PSILESDNSLNDEENNK	Q8IHQ2	PF11_0477	Y	N	1

Supplementary Table S8. *In vitro* physicochemical and pharmacokinetic properties of **2a**.[a]

	2a
Thermodynamic Solubility[b]	>3.4 mg/mL (>8 mM)
Plasma Stability (% Remaining after 2 h)	
Human	104%
Mouse	96.9%
Plasma Protein Binding (Fraction Unbound)	
Human	0.275
Mouse	0.213
Microsomal Stability (Cl_{int})	
Human	36.8 µL/min/mg protein
Mouse	26.9 µL/min/mg protein
Caco-2 Permeability (pH 7.4)	
P_{app} A-B	1.26×10^{-6} cm s^{-1}
P_{app} B-A	34.7×10^{-6} cm s^{-1}
Efflux Ratio (P_{app} B-A/ P_{app} A-B)	28

[a]All assays performed on free base. [b]Amorphous form.

Supplementary Table S9, related to Fig. 6: Changes in protein abundance due to NMT inhibition.

See attached Excel spreadsheet. Log_2 change in abundance is color-coded for proteins considered above the confidence limit ('significant').

Supplementary Methods

A. Chemical synthesis

General. All chemicals were purchased from Sigma-Aldrich Ltd (Gillingham, UK), Acros Organics (Geel, Belgium) and Alfa Aesar (Heysham, UK) and used without further purification. Moisture sensitive reactions were performed under nitrogen atmosphere using dried glassware, anhydrous solvents and standard syringe/septa techniques.

Silica gel normal phase column chromatography was performed on an Isolera (Biotage, UK) automated apparatus with SNAP silica cartridges (Biotage, UK). Mobile Phase consisted of *n*-hexane (solvent A) and ethyl acetate (solvent B) and standard gradient consisted of x % solvent B for 1 column volumes, x % to y % B for 10 column volumes then y % B for 2 column volume. x and y will be defined in the characterization section of the compound of interest.

Final compounds were purified by LC-MS.

LC-MS: RP-HPLC/MS on a Waters 2767 system equipped with a photodiode array and an ESI mass spectrometer using a XBridge Prep C18 (5 µm, 19 mm × 100 mm) column, equipped with an XBridge Prep C18 guard column (5 µm, 19 mm × 10 mm). The following elution method was used: Gradient of solvent A and solvent B (as above): 0-10 min 50-98 % B, 10-12 min 98 % B, 12-13 min 98 to 50 % B, 13-17 min 50 % B. Flow rate: 20 mL/min.

The purity of title compounds was verified by reverse phase LC-MS on a Waters 2767 system equipped with a photodiode array and an ESI mass spectrometer using a XBridge C18 (5 µm, 4.6 mm × 100 mm) column, equipped with an XBridge C18 guard column (5 µm, 4.6 mm × 20 mm). The following elution method was used: Gradient of solvent A and solvent B (as above): 0-10 min 5-98 % B, 10-12 min 98 % B, 12-13 min 98 to 5 % B, 13-17 min 5 % B. Flow rate: 1.2 mL/min. Purity of tested compounds was ≥ 95 %, unless specified.

^{1}H and ^{13}C NMR spectra were recorded on 400 MHz and 101 MHz respectively Bruker AV instruments at room temperature unless specified otherwise. In these cases ^{1}H and ^{13}C NMR spectra were recorded on 500 MHz and 126 MHz respectively Bruker AV instruments at room temperature and were referenced to residual solvent signals. Data are presented as follows: chemical shift in ppm, integration, multiplicity (br = broad, app = apparent, s = singlet, d = doublet, t = triplet, q = quartet, p = pentet, m = multiplet) and coupling constants in Hz.

Mass spectra were obtained from the Mass Spectrometry Service of Department of Chemistry, Imperial College London.

SPPS General. All reagents, amino acids and solvents were obtained from commercial sources (Sigma-Aldrich, Merck, AGTC Bioproducts) and were used without further purification.

Azidopropionic acid was prepared according to a published procedure.[4] HRMS was performed on Waters LCT Premier Spectrometer operating in W mode ES positive.

SPPS of AzKTB capture reagent. Biotin-PEG Novatag™ resin (0.47 mmol/g loading, 106.4 mg, 50.0 µmol, 1 eq) was swollen in DMF (2 mL, 30 min), Fmoc deprotected with 20 % v/v piperidine in DMF (2 mL, 10 min × 3) and washed with DMF, DCM and DMF sequentially. Fmoc-Lysine(Mmt)-OH (96.1 mg, 3 eq), HATU (57 mg, 3 eq) and DIPEA (52.3 µL, 6 eq) were dissolved in DMF (1 mL), added to the deprotected resin and the reaction was shaken for 2 h after which the procedure was repeated. All subsequent couplings, i.e. Fmoc-6-Ahx-OH, Fmoc-Gly-OH, Fmoc-Lys(Boc)-OH, Fmoc-Ala-OH, and Azidopropionic acid (all 5 eq) were performed using DIC/HOBt activation (5 eq each, 30 min x 2). Following the removal of Mmt protecting group with 1 % TFA in DCM (10 min x 4) and wash (DCM, DMF), TAMRA (43 mg, 2 eq) was activated for 10 min in DMF (1 mL) with DIC (15.7 mg, 2 eq) and HOAt (13.6 mg, 2 eq) and coupled to the peptidyl resin (2 h x 2). The crude product was then cleaved from the resin with 95 % TFA, 2.5 % water and 2.5 % triisopropylsilane (3 h) and precipitated with cold TBME. The solids were pelleted by centrifugation (15 min, 3000 g, 4 °C) and washed three times with TBME. The pelleted product was dried and purified by semi preparative LC-MS over a gradient of MeOH (0.1% FA) in water (0.1% FA) (2-98 %, 15 min), with detection over 100–600 nm. The product was obtained by lyophilization as a bright pink amorphous solid (12 mg, 17 % yield). HRMS m/z (ESI), calculated for $C_{71}H_{104}N_{16}O_{15}S$ ($[M + 2H]^{2+}$) 727.3873, found 727.3892.

B. Synthesis and characterization of compounds

Series 1: inhibitors 1a-c

Compounds **1a-c** were first reported by Brand *et al.*[5, 6] and were synthesized using methods described previously.[1]

Ethyl-3-hydroxybenzo[*b*]thiophene-2-carboxylate 3

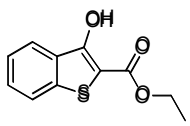

To a solution of methyl-2-mercaptobenzoate (1.63 mL, 11.9 mmol, 1.0 equivalents) and ethyl bromoacetate (1.32 mL, 11.9 mmol, 1.0 equivalents) in dry THF (130 mL) at 0 °C was added potassium *tert*-butoxide (5.14 g, 71.3 mmol, 6.0 equivalents) gradually over 2 mins. The reaction mixture was stirred and allowed to warm to room temperature over 15 mins, quenched with 2 M HCl to pH 2 and diluted with 75 mL water. **3** was immediately extracted with 3 × 75 mL portions of EtOAc. The organic layers were combined, washed with 75 mL brine, dried over $MgSO_4$ and concentrated under reduced pressure to give desired product **3** as a yellow solid (2.32 g, 88 %). ^{1}H NMR ($CDCl_3$, δppm) 10.21 (1H, brs), 7.94 (1H, d, *J* = 8.0 Hz), 7.74 (1H, d, *J* = 8.0 Hz), 7.50 (1H, ddd, *J* = 8.0, 7.5, 1.4 Hz), 7.44–7.37 (1H, m), 4.43 (2H, q, *J* = 7.1 Hz), 1.43 (3H, t, *J* = 7.1 Hz).

tert-Butyl-4-((2-(ethoxycarbonyl)benzo[_b_]thiophen-3-yl)oxy)piperidine-1-carboxylate 4

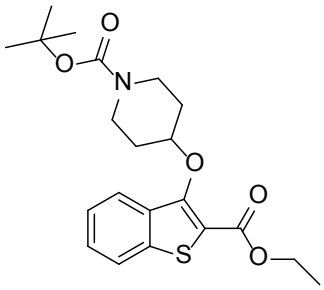

To a solution of **3** (2.70 g, 12.2 mmol, 1.0 equivalents) in THF (30 mL) was added *tert*-butyl-4-hydroxypiperidine-1-carboxylate (4.89 g, 24.3 mmol, 2.0 equivalents) and triphenylphosphine (6.38 g, 24.3 mmol, 2.0 equivalents). The reaction mixture was stirred under nitrogen for 20 min, cooled to 0 °C and diisopropyl azodicarboxylate (4.79 mL, 24.3 mmol, 2.0 equivalents) in THF (10 mL) was added drop-wise over 5 min. Reaction mixture was allowed to warm to room temperature and stirred for 1.5 h, concentrated under reduced pressure and the crude product purified by flash column chromatography (100g SNAP cartridge, 2% to 18% B, R_f = 7 column volumes) to give **4** as a pink oil (4.77 g, 97 %). ^{1}H NMR ($CDCl_3$, δppm) 7.86 (1H, d, *J* = 7.9 Hz), 7.74 (1H, d, *J* = 8.0 Hz), 7.47 (1H, ddd, *J* = 8.0, 7.8, 0.8 Hz), 7.39 (1H, dd, *J* = 7.9, 7.8 Hz), 4.79 – 4.69 (1H, m), 4.38 (2H, q, *J* = 7.2 Hz), 4.01–3.86 (2H, m), 3.20–3.07 (2H, m), 2.05–1.95 (2H, m), 1.91–1.79 (2H, m), 1.48 (9H, s), 1.41 (3H, t, *J* = 7.2 Hz).

tert-Butyl 4-((2-(hydrazinecarbonyl)benzo[_b_]thiophen-3-yl)oxy)piperidine-1-carboxylate 5

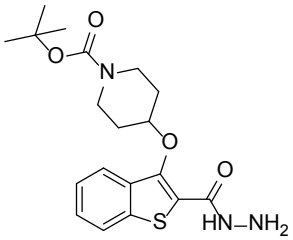

To a solution of **4** (300 mg, 0.74 mmol, 1.0 equivalents) in EtOH (1 mL) was added hydrazine monohydrate (145 µL, 2.96 mmol, 4.0 equivalents). The reaction mixture was heated under refluxing conditions for 24 h, then concentrated under reduced pressure yielding **5** as a yellow oil (217 mg, 75 %). ^{1}H NMR ($CDCl_3$, δppm) 7.79 (1H, d, *J* = 7.6 Hz), 7.74 (1H, d, *J* = 7.2 Hz), 7.48 – 7.37 (2H, m), 4.58 (1H, tt, *J* = 9.8, 4.1 Hz), 4.13 – 4.04 (2H, m), 2.95 – 2.82 (2H, m), 2.14 – 2.05 (2H, m), 1.92 – 1.78 (2H, m), 1.48 (9H, s).

Ethyl 3-acetyl-4-oxopentanoate 6[7]

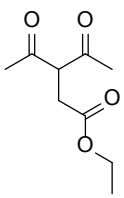

To a solution of sodium hydride (576 mg, 24.0 mmol, 1.2 equivalents) in anhydrous THF (30 mL) cooled to 0 °C was added pentane-2,4-dione (2.05 mL, 20.0 mmol, 1.0 equivalents) in anhydrous THF (40 mL) and reaction stirred for 1 h. Ethyl bromoacetate (2.66 mL, 24.0 mmol, 1.2 equivalents) in anhydrous THF (30 mL) was then added and the reaction mixture was stirred for 18 h. The reaction mixture was then washed with saturated $NH_4Cl_{(aq)}$ (100 mL) and aqueous layer was back-extracted with EtOAc (100 mL). Combined organic layers were washed with brine (100 mL), dried over $MgSO_4$ and concentrated under reduced pressure, yielding **6** as a yellow oil (2.90 g, 78 %). Mixture of diketone:enol tautomers 2:1 as observed by NMR in $CDCl_3$ at room temperature; Diketone ^{1}H NMR ($CDCl_3$, δppm);. 4.20 – 4.12 (3H, m), 2.90 (2H, d, *J* = 7.3 Hz), 2.29 (6H, s), 1.31 – 1.25 (3H, m); Enol ^{1}H NMR ($CDCl_3$, δppm); 4.22 – 4.08 (2H, m), 3.25 (2H, s), 2.17 (6H, s), 1.32 – 1.23 (3H, m).

Ethyl 2-(1,3,5-trimethyl-1*H*-pyrazol-4-yl)acetate 7[8]

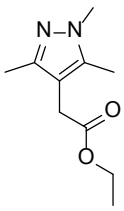

To a solution of **6** (400 mg, 2.15 mmol, 1.0 equivalents) in AcOH (3 mL) was added methyl hydrazine (125 µL, 2.37 mmol, 1.1 equivalents) drop-wise and reaction stirred at room temperature for 3 h. Reaction mixture was concentrated under reduced pressure, yielding **7** as a colorless oil (349 mg, 73 %). ^{1}H NMR ($CDCl_3$, δppm); 4.15 (2H, q, *J* = 7.1 Hz), 3.74 (3H, s), 3.35 (2H, s), 2.22 (6H, s), 1.28 (3H, t, *J* = 7.1 Hz).

2-(1,3,5-Trimethyl-1*H*-pyrazol-4-yl)acetic acid 8

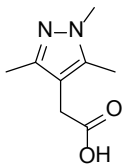

To a solution of **7** (300 mg, 1.53 mmol, 1.0 equivalents) in MeOH (3 mL) was added lithium hydroxide monohydrate (642 mg, 15.3 mmol, 10.0 equivalents) and reaction stirred at room temperature for 18 h. Reaction mixture was diluted with water (20 mL) and acidified with 2.0M $HCl_{(aq)}$ to pH 4, then **8** was extracted with EtOAc (3 x 20 mL). Combined organic layers were then dried over Na_2SO_4 and concentrated under reduced pressure, yielding **8** as a pink solid (130 mg, 51 %). ^{1}H NMR ($CDCl_3$, δppm); 3.80 (3H, s), 3.41 (2H, s), 2.24 (3H, s), 2.23 (3H, s).

***tert*-Butyl 4-((2-(2-(2-(1,3,5-trimethyl-1*H*-pyrazol-4-yl)acetyl)hydrazinecarbonyl)benzo[*b*]thiophen-3-yl)oxy)piperidine-1-carboxylate 9**

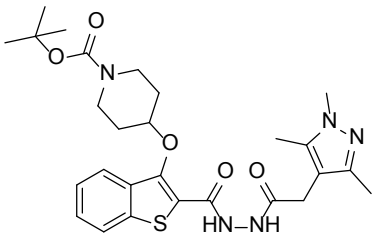

To a solution of **5** (48 mg, 0.12 mmol, 1.0 equivalents) in THF:DMF (4:1 *v*/*v*, 0.6 mL) was added hydroxybenzotriazole (8 mg, 0.06 mmol, 0.5 equivalents), 1-ethyl-3-(3-dimethylaminopropyl) carbodiimide hydrochloride (28 mg, 0.15 mmol, 1.3 equivalents) and **8** (25 mg, 0.15 mmol, 1.3 equivalents). Reaction mixture stirred at room temperature for 18 h, then diluted with 1.0 M $NaOH_{(aq)}$ (4 mL) and **9** extracted with EtOAc (2 x 5 mL). Combined organic layers were washed with brine (5 mL), dried over Na_2SO_4 and concentrated under reduced pressure, yielding **9** as an orange oil which was used without further purification (43 mg, 66 %). ^{1}H NMR ($CDCl_3$, δppm); 9.75 (1H, d, *J* = 6.2 Hz), 7.89 – 7.72 (3H, m), 7.53 – 7.37 (2H, m), 4.75 – 4.65 (1H, m), 4.12 – 4.06 (2H, m), 3.76 (3H, s), 3.46 (2H, s), 2.86 – 2.82 (2H, m), 2.26 (6H, s), 2.14 – 2.09 (2H, m), 1.99 – 1.87 (2H, m), 1.48 (9H, s).

2-(3-(Piperidin-4-yloxy)benzo[*b*]thiophen-2-yl)-5-((1,3,5-trimethyl-1*H*-pyrazol-4-yl)methyl)-1,3,4-oxadiazole 2a

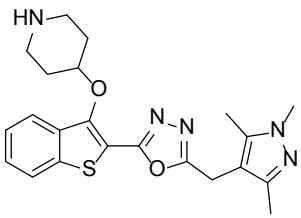

To a solution of **9** (66 mg, 0.12 mmol, 1.0 equivalents) and 1,2,2,6,6-pentamethylpiperidine (47 µL, 0.26 mmol, 2.2 equivalents) in DCM (1 mL) was added *m*-toluenesulfonyl chloride (25 mg, 0.13 mmol, 1.1 equivalents) and the reaction mixture was stirred at room temperature for 18 h. The reaction mixture was then diluted with a

further 2 mL dichloromethane, washed with water (2 mL), 1.0M $NaOH_{(aq)}$ (2 mL), brine (2 mL), dried over $MgSO_4$ and concentrated under reduced pressure. The *tert*-butoxycarbonyl group was removed without further purification by dissolving the crude reaction product (36 mg) in DCM (1 mL), followed by the addition of TFA (100 µL). The solution was stirred at room temperature for 2 h, concentrated under reduced pressure and purified by LC-MS yielding **2a** as a yellow solid (9 mg, 17 %). R_t = 7.1 min; ^{1}H NMR (CD_3OD, δppm); 8.47 (1H, brs), 7.99 – 7.88 (2H, m), 7.61 – 7.45 (2H, m), 4.81 (1H, tt, *J* = 7.2, 4.1 Hz), 4.12 (2H, s), 3.72 (3H, s), 3.56 (2H, ddd, *J* = 12.1, 7.5, 4.1 Hz), 3.11 (2H, ddd, *J* = 12.5, 7.5, 4.1 Hz), 2.29 (3H, s), 2.22 (3H, s), 2.21 – 2.04 (4H, m); ^{13}C NMR (CD_3OD, δppm); 170.17, 160.26, 147.99, 134.99, 139.01, 134.93, 134.27, 128.98, 126.59, 124.49, 123.45, 120.38, 109.98, 77.73, 45.42, 42.37, 36.01, 29.56, 20.79, 9.52; ESI HRMS, found 424.1801 ($C_{22}H_{26}N_5O_2S$, $[M + H]^+$, requires 424.1807).

Ethyl 2-(3,5-dimethyl-1*H*-pyrazol-4-yl)acetate 10[7]

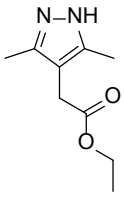

To a solution of **6** (400 mg, 2.15 mmol, 1.0 equivalents) in methanol (3 mL) was added hydrazine monohydrate (157 µL, 3.23 mmol, 1.5 equivalents) and reaction stirred at room temperature for 3 h. Reaction mixture was concentrated under reduced pressure, yielding **10** as a colorless oil (349 mg, 83 %). ^{1}H NMR ($CDCl_3$, δppm); 7.38 (1H, brs), 4.13 (2H, q, *J* = 7.1 Hz), 3.36 (2H, s), 2.25 (6H, s), 1.25 (3H, t, *J* = 7.1 Hz).

2-(3,5-Dimethyl-1*H*-pyrazol-4-yl)acetic acid 11

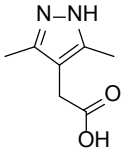

To a solution of **10** (225 mg, 1.24 mmol, 1.0 equivalents) in MeOH (3 mL) was added lithium hydroxide monohydrate (521 mg, 12.4 mmol, 10.0 equivalents) and reaction stirred at room temperature for 18 h. Reaction mixture was diluted with water (20 mL) and acidified with 2.0 M $HCl_{(aq)}$ to pH 4, then **11** was extracted with EtOAc (3 x 20 mL). Combined organic layers were then dried over sodium sulfate and concentrated under reduced pressure, yielding **11** as a white solid (23 mg, 12 %). ^{1}H NMR ($CDCl_3$, δppm); 3.40 (2H, s), 2.31 (3H, s), 2.18 (3H, s).

***tert*-Butyl 4-((2-(2-(2-(3,5-dimethyl-1*H*-pyrazol-4-yl)acetyl)hydrazinecarbonyl)benzo[*b*]thiophen-3-yl)oxy)piperidine-1-carboxylate 12**

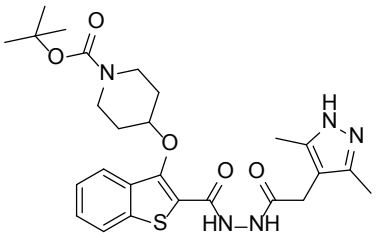

To a solution of **5** (48 mg, 0.12 mmol, 1.0 equivalents) in THF:DMF (4:1 *v*/*v*, 0.6 mL) was added hydroxybenzotriazole (8 mg, 0.06 mmol, 0.5 equivalents), 1-ethyl-3-(3-dimethylaminopropyl) carbodiimide hydrochloride (28 mg, 0.15 mmol, 1.3 equivalents) and **11** (23 mg, 0.15 mmol, 1.3 equivalents). Reaction mixture stirred at room temperature for 18 h, then diluted with 1.0 M $NaOH_{(aq)}$ (4 mL) and **12** extracted with EtOAc (2 x 5 mL). Combined organic layers were washed with brine (5 mL), dried over Na_2SO_4 and concentrated under reduced pressure, yielding **12** as a

yellow solid which was used without further purification (30 mg, 48 %). ^{1}H NMR ($CDCl_3$, δppm); 7.86 – 7.72 (2H, m), 7.51 – 7.37 (2H, m), 4.80 – 4.65 (1H, m), 4.16 – 4.04 (2H, m), 3.48 (2H, s), 2.89 – 2.81 (2H, m), 2.29 (3H, s), 2.15 – 2.09 (2H, m), 2.06 (3H, s), 1.92 – 1.83 (2H, m), 1.48 (9H, s).

2-((3,5-Dimethyl-1*H*-pyrazol-4-yl)methyl)-5-(3-(piperidin-4-yloxy)benzo[*b*]thiophen-2-yl)-1,3,4-oxadiazole 2b

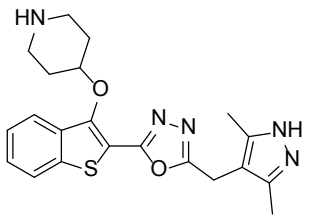

To a solution of **12** (62 mg, 0.12 mmol, 1.0 equivalents) and 1,2,2,6,6-pentamethylpiperidine (47 µL, 0.26 mmol, 2.2 equivalents) in DCM (1 mL) was added *m*-toluenesulfonyl chloride (25 mg, 0.13 mmol, 1.1 equivalents) and the reaction mixture was stirred at room temperature for 18 h. The reaction mixture was then diluted with a further 2 mL DCM, washed with water (2 mL), 1.0 M $NaOH_{(aq)}$ (2 mL), brine (2 mL), dried over $MgSO_4$ and concentrated under reduced pressure. The *tert*-butoxycarbonyl group was removed without further purification by dissolving the crude reaction product (10 mg) in DCM (1 mL), followed by the addition of TFA (100 µL). The solution was stirred at room temperature for 2 h, concentrated under reduced pressure and purified by LC-MS yielding **2b** as a yellow solid (4 mg, 8 %). R_t = 7.7 min; ^{1}H NMR (CD_3OD, δppm); 7.96 – 7.88 (2H, m), 7.59 – 7.46 (2H, m), 4.77 (1H, tt, *J* = 7.3, 3.8 Hz), 4.13 (2H, s), 3.53 (2H, ddd, *J* = 12.0, 7.1, 4.1 Hz), 3.13 – 3.03 (2H, m), 2.27 (6H, s), 2.21 – 2.01 (4H, m); ESI HRMS, found 410.1653 ($C_{21}H_{24}N_5O_2S$, $[M + H]^+$, requires 410.1651). 90% Pure by LC-MS.

C. Protein crystallography

Protein crystallization of the binary complex PvNMT-YnMyrCoA or the ternary complex PvNMT with the non-hydrolysable myristoyl-CoA analogue NHMCoA and compounds **1a** or **2a** was essentially as described previously.[9] X-ray diffraction data were collected on the synchrotron beam lines i04 and i04-1 at Diamond Light Source, Didcot, and processed using XDS[10] and SCALA[11] implemented within *xia2*.[12] Data collection and refinement statistics are summarized in Supplementary Table S1. For R_{free} calculations, 5% of the data were excluded. Rigid body refinement using maximum likelihood methods implemented in REFMAC[13] using the protein chains of 4TST.pdb[9] as a starting model was followed by refinement using anisotropic temperature factors, interspersed with cycles of model building and adjustment using COOT.[14] Complete chains (corresponding to residues 27-410, numbering as in full-length protein) can be traced for two of the three molecules in the asymmetric unit. N-terminal residues (derived from the purification tag) in all three chains and loop residues 227-242 in chain C have not been modeled and these are assumed to be disordered. The final refined protein structure model displays good geometry with only 0.3% of the amino acid residues (corresponding to Phe336 in all three chains) falling in a non-ideal region of a Ramachandran plot. The coordinates and structure factor files have been deposited in

the Protein Data Bank under the accession codes 2ync (PvNMT-YnMyrCoA), 2ynd (PvNMT-NHMCoA-**1a**) and 2yne (PvNMT-NHMCoA-**2a**), respectively.

D. Parasite culture and assays

Parasites were cultured as described previously and schizont stages purified using magnetic columns (MACS),[15] before returning to culture for 2-4 h and synchronizing the newly invaded ring-stage parasites with 5 % D-sorbitol,[16] one cycle prior to use.

Metabolic tagging of parasites. For tagging, assays were set up using parasites at 40 h post invasion (based on initial Giemsa-stained smear observations) and diluted to ~10 % parasitemia. A haematocrit of 4 % was used to increase the total number of parasites harvested. To each culture the required volume of YnMyr, YnPal, AHA or CHX was added from stocks, along with any inhibitors. DMSO controls were set up in parallel. Cultures were re-incubated (37 °C) for a further 5 h. Parasite cultures were pelleted and the red cells lysed in 1 × culture volume of 0.15 % saponin in PBS. Pellets were washed twice in the same buffer to remove red cell proteins. Parasite proteins were extracted using 1 % Triton X-100 in 10 mM Na_2PO_4 pH 8.2 with protease inhibitors (EDTA-free, Roche) and incubated overnight at 4 °C with rotation. Extracts were pelleted and the concentration of protein in the supernatant determined by DC protein assay (Bio-Rad).

Inhibition studies (EC_{50} determination). Trophozoite-stage cultures (~24 h post invasion) were added (0.2 % parasitemia, 2 % hematocrit) to 96-well plates containing inhibitor in duplicate wells, final volume 100 µl. Inhibitor concentrations ranged from 10 - 0.004 µM. Cultures were incubated in gassed humidity chambers (90 % N_2, 5 % CO_2 and 5 % O_2) at 37 °C for a further 96 h; inhibitor and medium were refreshed at 48 h. After 96 h, cultures were lysed and the DNA stained by adding 25 µl lysis buffer (20 mM Tris.HCl pH 8.0, 2 mM EDTA, 0.16 % saponin, 1.6 % Triton X-100) containing 0.1 % Sybr Green to each 100 µl well. Plates were incubated 3-24 h in dark at room temperature before reading on a fluorimeter at 520 nm.

Phenotype studies. Parasite assays to determine the effect of inhibitor on development and invasion ("pseudoschizont" analysis by thin smear, Western blot and LC-MS/MS proteomics) commenced with addition of inhibitor **1a** (1 µM) or DMSO vehicle (control) to synchronized ring stages 0-4 h post-invasion at 4 % hematocrit and 5.3 % parasitemia (100 mL cultures). Parasites were cultured for different times (as indicated in **Fig. S20**), then thin films were prepared, methanol-fixed and stained with Giemsa's reagent prior to microscopic observation. Thin films were also used for immunofluorescence analysis (see Section 2.8). At 45 h PI, an aliquot of each sample was taken for parasite lysis and proteomic analysis by Western blot and LC-MS/MS (sections 2.6 and 2.7). Parasites were pelleted and the red cells lysed in 1 × culture volume of 0.15 % saponin in PBS. Pellets were washed twice in the same buffer to remove red cell proteins and parasites lysed in 1 % TX100, 10 mM Na_2PO_4 pH 8.2.

Wash-out experiment. To study whether removal of inhibitor rescued parasite growth, cultures were set up at ring stages 0-4 h post-invasion at 2 % hematocrit and ~1 % parasitemia in the presence of NMT inhibitor (1 μM **1a**) or DMSO vehicle. Parasites were cultured to 45 h PI, medium was exchanged for medium containing either NMT inhibitor (1 μM **1a**) or DMSO vehicle (45 h wash-out), and parasite life stages analyzed with Giemsa's reagent (as described above) at 55 h PI.

E. CuAAC labeling and pull-down

Protein lysates were adjusted to 1 mg/mL with lysis buffer; premixed click reagents (100 μM AzTB, 1 mM $CuSO_4$, 1 mM TCEP, 100 μM TBTA, final concentrations) were added as described previously[2] and samples vortexed for 1 h RT, then quenched by the addition of 10 mM EDTA, followed by 10 volumes of ice-cold MeOH. Samples were left at -80 °C overnight and then proteins pelleted by centrifugation at 17,000 ×g for 20 min at 4°C. Pellets were washed with ice-cold MeOH, then air-dried for ~15 min. Protein was resuspended in 2 % SDS, 10 mM EDTA in PBS ("Resuspension Buffer"). 4 × sample loading buffer (NuPAGE LDS sample buffer) with 2-mercaptoethanol (4 % final) was added and proteins heated for 3 min at 95 °C prior to SDS-PAGE.

Pull-down. After click chemistry and precipitation, protein was resuspended at 10 mg/mL in Resuspension Buffer, and then diluted to 1 mg/mL with PBS. DTT (from a fresh 100 × stock in water) was added to give a final concentration of 1 mM. Proteins were incubated with Dynabeads® MyOne™ Streptavidin C1 (pre-washed 3 × 0.2 % SDS in PBS) for 1.5-2 h at RT with rotation. Following removal of the supernatant, beads were washed with 3 × 0.2 % SDS in PBS, then boiled for 10 mins in sample loading buffer elute bound proteins. Aliquots of supernatant and pre-PD sample were also taken for gel analysis.

Hydroxylamine cleavage of thioesters prior to pull-down. Following click reaction and precipitation, proteins were resuspended at 10 mg/mL in Resuspension Buffer, then diluted to 2 mg/mL with PBS and treated with 1 M freshly neutralized NH_2OH (50 % solution in water, neutralized to pH ~7 with conc. HCl) for 1 hour at RT with vortexing. Samples were then diluted with PBS to 1 mg/mL for pull-down.

Base cleavage of esters prior to pull-down. Following click reaction and precipitation, proteins were resuspended at 10 mg/mL in Resuspension Buffer, then diluted to 2 mg/mL with PBS and treated with 0.2 M NaOH for 1 hour at RT with vortexing. Samples were then neutralized with an equivalent volume of HCl and diluted with PBS to 1 mg/mL for pull-down.

Gel-based fluorescence analysis. Samples were separated by SDS-PAGE and the gel soaked in fixing solution (10 % AcOH, 40 % MeOH), then rinsed in water for in-gel fluorescent imaging: gels were scanned with Cy3 filters to detect the TAMRA fluorophore using an Ettan DIGE scanner, GE

Healthcare. Molecular weight markers (Precision Plus All Blue Standards, Bio-Rad) were detected with Cy5 filters.

ImageJ was used for quantification of fluorescent bands. A thin rectangle was dropped down the length of the lane and the 'gel analyzer' function used to plot the profile of intensity down the lane (with averaging across horizontally). The signal was measured by integrating the area under each band of interest and normalizing relative to no inhibition (YnMyr). Any background (from DMSO, no YnMyr sample) was subtracted. Total protein loading was checked by Coomassie or Western blot for housekeeper protein BiP. In-cell tagging IC_{50} (TC_{50}) was calculated by fitting data to a background-corrected IC50 function using GraFit 7.0 (Erithacus Software Ltd, UK).

F. Immunoblot analysis

For immunoblotting, proteins were transferred to nitrocellulose membranes, membranes were blocked (5 % dried skimmed milk in TBS 0.1 % Tween-20), then incubated with the appropriate primary, then secondary antibodies in blocking solution, and developed with Luminata Crescendo Western HRP substrate (Millipore) according to the manufacturer's instructions and on a Fujifilm LAS 3000 imager.

Primary antibodies: anti-GAP45 (rabbit),[17] anti-CDPK1 (rabbit),[18] anti-$MSP1_{19}$ (rabbit),[19] anti-MTIP (rabbit)[20] and anti-BiP (rat; MR4) were used at 1:1000-2000 in blocking solution. Anti-ARO and anti-ARF (see below) were used at 1:500 in blocking solution. Secondary antibodies: goat anti-rabbit IgG-HRP secondary (Invitrogen) and donkey anti-rat IgG-HRP secondary (SouthernBiotech) were used at 1:10000.

Production of antibodies. Anti-ARO (PFD0720w) antibodies were produced by expression of full length protein fused to GST in *E. coli* followed by protein purification, removal of the GST tag and rabbit immunization with the ARO protein (Harlan). Anti-ARF antibodies were produced to a synthetic ARF peptide by rabbit immunization (Pepceuticals).

G. MS proteomics for YnMyr target identification

Preparation for MS-based proteomics. Proteins were captured by CuAAC and affinity-enriched as detailed above with the following modifications: NeutrAvidin agarose resin (Thermo Scientific) was used in place of the magnetic Dynabeads due to increased stability of the resin during on-bead reduction and alkylation of proteins. Beads were stringently washed following pull-down: 3 × 1 % SDS in PBS, 3 × 4M Urea in 50 mM TEAB, 2 × water, 3 × 50 mM TEAB (triethylammonium bicarbonate). Beads were stored at 4 °C in 50 mM TEAB solution.

For gel-based analysis, proteins were eluted from beads by boiling in sample loading buffer containing 2-mercaptoethanol, and then separated on a pre-cast gel (NuPAGE Novex 10 % Bis-

Tris Gel, 1.5-mm thick). Proteins were stained with Instant Blue (Expedeon) for 2 h, washed with water and the gel cut to give 9 portions, which were stored frozen in 50 mM TEAB before digest.

On-bead reduction, alkylation and digest. Beads were spun at 6000 g for 5min, excess liquid discarded and resuspended in 50 µL of 50 mM TEAB and 6 µL of acetonitrile. Samples were reduced (2.8 µL of 100 mM dithiothreitol in 50 mM TEAB) at 60 °C for 30 minutes and allowed to cool to room temperature. Cysteines were alkylated (5.9 µL of 100 mM iodoacetamide in 50 mM TEAB) at room temperature for 30 min in the dark. Trypsin (5 µg in 25 µL of 50 mM TEAB) was added to the beads and samples were placed on a shaker and digested overnight at 37 °C. Each sample (beads and liquid) was transferred to a MobiSpin Column F (2B Scientific, UK) and spun at low speed (<4500 g). The flow through was evaporated to dryness (Savant DNA 120 concentrator, Thermo Scientific) and resuspended using 20 µL of a 10 fmol/µL yeast alcohol dehydrogenase tryptic digest standard (Waters, UK).

In-gel reduction, alkylation and digest. Each slice was destained using 200 mM TEAB/20 % acetonitrile, followed by reduction (10 mM DTT) at 60 °C for 30 minutes, alkylation (100 mM iodoacetamide) at room temperature for 30 minutes in the dark and enzymatic digestion (0.1 µg sequencing grade modified porcine trypsin) overnight at 37 °C. The liquid was evaporated to dryness and resuspended using 20 µL of a 10 fmol/µL yeast alcohol dehydrogenase tryptic digest standard (Waters, UK).

LC-MS/MS runs. LC-MS/MS was carried out using an RSLCnano HPLC system (Dionex, UK) and an LTQ-Orbitrap-Velos mass spectrometer (Thermo Scientific). Samples were loaded at high flow rate onto a reverse-phase trap column (0.3 mm i.d. x 1 mm), containing 5 µm C18 300 Å Acclaim PepMap media (Dionex) maintained at a temperature of 37 °C. The loading buffer was 0.1 % formic acid / 0.05 % trifluoroacetic acid in water. Peptides were eluted from the trap column at a flow rate of 0.3 µl/min and through a reverse-phase capillary column (75 µm i.d. x 250 mm) containing Symmetry C18 100 Å media (Waters, UK) that was manufactured in-house using a high pressure packing device (Proxeon Biosystems, Denmark). The output from the column was sprayed directly into the nanospray ion source of an LTQ-Orbitrap-Velos mass spectrometer set to acquire a single microscan FTMS scan event at 60000 resolution over the m/z range 350-1250 Da in positive ion mode. Accurate calibration of the FTMS scan was achieved using a background ion lock mass for polydimethylcyclosiloxane (445.120025 Da). Subsequently up to 10 data dependent HCD MS/MS were triggered from the FTMS scan and performed in the LTQ-Velos ion-trap. The isolation width was 2.0 Da, normalized collision energy 45.0, Activation time 0.1 ms. Dynamic exclusion was enabled.

LC-MS/MS data analysis. The .raw data file obtained from each LC-MS/MS acquisition was processed using the Raw2MSM application.[21] The resulting .msm files were searched using Mascot (version 2.2.04, Matrix Science Ltd.)[22] against a database containing the

UniProtKB/Swissprot[23] accessions for *Plasmodium falciparum* and *Homo sapiens*. The peptide tolerance was set to 5 ppm and the MS/MS tolerance was set to 0.02 Da. Fixed modifications were set as carbamidomethyl cysteine with variable modifications as oxidised methionine. The enzyme was set to Trypsin/P and up to 3 missed cleavages were allowed. A decoy database search was performed.

Data were further processed using Scaffold (version 3.6.02, Proteome Software).[24] The Mascot .dat files were imported and searched using X!Tandem (version 2006.9.15.4, The Global Proteome Machine Organization).[25] PeptideProphet[26] and ProteinProphet[27] (Institute for Systems Biology) probability thresholds of 95 % were calculated from each of the Mascot and X!Tandem decoy searches and Scaffold was used to calculated an improved 95 % peptide and protein probability threshold based on the data from the two different search algorithms, resulting in a peptide false discovery rate of 0.0 %. Protein identifications were required to contain at least 2 peptides exceeding 95 % probability giving a calculated protein false discovery rate of 0.0 %.

Proteomic data processing. Data imported into Scaffold were further elaborated in Microsoft Excel. Proteins with spectral counts <4-fold enriched in YnMyr sample compared to the DMSO control were discarded as non-specific binders. Proteins whose enrichment was reduced or eliminated in the samples that had been treated with NaOH compared to non-treated samples were grouped as 'Base sensitive'. Bioinformatic tools PredGPI[28] (http://gpcr.biocomp.unibo.it/predgpi/) and GPI-SOM (http://gpi.unibe.ch/) used to assess whether these proteins were likely to be GPI-anchored. Proteins with counts that were maintained or increased with base treatment were assigned as 'Base insensitive' and separated into those that had an N-terminal glycine, and are therefore potential NMT substrates, and those that did not.

Identification of the modified peptide with AzKTB. Proteins were captured by CuAAC as before with the following modifications: CuAAC reaction was carried out for 2 hours and with AzKTB in place of AzTB. Proteins were precipitated following CuAAC via a modified chloroform/methanol precipitation procedure: 4 volumes of MeOH, 1 vol. $CHCl_3$, 3 vol. H_2O were added to the sample, which was centrifuged at 17,000 ×g for 5 min to pellet proteins at the interface. Both layers were then removed simultaneously, the pellet resuspended in 0.2 % SDS/PBS to the original volume and the precipitation procedure repeated. The pellet was then washed twice with MeOH. Resuspension, affinity enrichment and preparation for LC-MS/MS were performed as before with the following modifications: beads were washed with 15 % ACN in TEAB following digest and this wash combined with the supernatant from on-bead digest to improve recovery of modified peptides.

The data were processed with MaxQuant version 1.3.0.5, and the peptides were identified from the MS/MS spectra searched against the UniProtKB *Plasmodium falciparum* (isolate 3D7) database (ver. 22/05/2012) using the Andromeda search engine. Cysteine carbamidomethylation was used

as a fixed modification and methionine oxidation, protein N-terminal acetylation and N-terminal addition of 520.3373 (corresponding to the triazole adduct) as variable modifications. For the identification, the false discovery rate was set to 0.01 for peptides, proteins and sites, the minimum peptide length allowed was five amino acids, and the minimum number of unique peptides allowed was set to one. Other parameters were used as pre-set in the software.

H. Proteomics analysis of inhibited parasites

Equal protein quantities in whole cell lysate of parasites (45 h PI) cultured in presence of NMT inhibitor (1 μM **1a**) or DMSO vehicle were processed by FASP™,[29] subjected to tryptic digest and analysed by nanoLC-MS/MS (n = 4). Protein identification and label-free quantification in MaxQuant produced a list of 1900 parasite proteins; data were filtered in Perseus v1.4.1.3 for completeness (minimum 3 quantifications per protein per group) yielding 1181 proteins for which relative abundance was determined using a two-tailed t-test (FDR = 0.05, 250 randomizations).

I. Immunofluorescence analysis

Indirect immunofluorescence assay (IFA) was performed on air dried thin smears of parasites on glass slides, following fixation in 4 % formaldehyde for 15 min and permeabilization for 5 min in 0.1 % Nonidet P40 in PBS, before blocking in 3 % BSA in PBS overnight at 4 °C. Rabbit anti-GAP45 antibody[17] diluted in 3 % BSA in PBS was added for 1 h at room temperature (RT) and then the slides were washed in PBS for 30 min, before incubation with secondary AlexaFluor-488 labelled antibodies (Invitrogen) at 1:5000. Nuclei were stained with DAPI (4',6-diamidino-2-phenylindole). Slides were mounted in Vectashield and viewed on a Zeiss Axioplan 2 imaging system with Plan Apochromat 100x/1.4 oil immersion objective. Images were captured using Axiovision 4.6.3 software and edited using Adobe Photoshop.

J. Enzyme Assays

Substrate kinetic assay for NMT. Kinetic assays for YnMyr-CoA or Myr-CoA with PvNMT or PfNMT were carried using a 7-diethylamine-3-(4'maleimidylphenyl)-4-methylcoumarin (CPM) fluorescence assay, as described previously by Goncalves *et al.*[1, 9] For PfNMT the final enzyme concentration was modified (final concentration 400 ng/mL); the peptide substrate used was GSNKSKPKDASQRRR-NH_2.

Enzyme assay for inhibitor testing. All IC_{50} determinations were carried out using a CPM fluorescence assay, as described by Goncalves *et al.*[1, 9] with the modifications described above.

Data were elaborated using Microsoft Office Excel 2010 and IC_{50} values were determined using GraFit 7.0 (Erithacus Software Ltd, UK) by non-linear regression fitting, which were then quoted as K_i as defined below.

K_i Calculations. K_i values were calculated from the experimentally determined IC_{50} values, the substrate concentration ([S]) and the Michaelis-Menten constant (K_m) as described by the Cheng-Prusoff equation.[30]

K. *In vivo* mouse experiments with *P. berghei*

Ethics statement. All animal work was approved by the United Kingdom Home Office and passed an ethical review process. All work carried out was in compliance with European Directive 86/609/EEC for the protection of animals used for experimental purposes and in accordance with the United Kingdom "Animals (Scientific Procedures) Act 1986". The project license permit number is 40/3344. Tuck's Original (TO) (Harlan) outbred female mice weighing 22-28 g were used for all experiments.

Compound toxicity tests. Naive mice were treated with **2a** at 50 mg/kg through intra-peritoneal injection twice a day and observed for 24 hours to check for changes in behaviour or neurological symptoms.

Compound efficacy tests. *Plasmodium berghei*, GFP ANKA 507 clone 1 strain,[31] ($1x10^7$) was dissolved in 150 µL PBS and delivered through intra-peritoneal injection into three experimental mice (M1-M3) and two control mice (M4, M5). 48 hours after parasite injection, the experimental group were treated with drug (50 mg/kg in 150 µL PBS) twice daily for three days. Blood smear to determine parasite load was performed daily by taking drop of tail blood and staining the blood smear with Giemsa. 5-10 fields with 1500-2000 total RBCs were counted and numbers of cells infected with parasites was determined. Percentage parasitemia was then determined for both control and experimental group.

L. Pharmacokinetic experiments

All pharmacokinetic experiments were performed by Cyprotex (http://www.cyprotex.com/home/).

Thermodynamic Solubility. Compound (2.5 mg of solid; n=1) was weighed in a clear glass vial and buffer (0.5 mL) added (typically phosphate buffered saline pH 7.4). The solution was agitated at ambient temperature overnight using a vial roller system. The solution was then filtered (0.45 µm pore size; without pre-saturation). Duplicate aliquots (50 µL) were sampled from the filtrate and diluted with one volume of 0.1 N hydrochloric acid and methanol (1:1 v/v) before analysis by HPLC-UV. A standard was prepared in DMSO at 10 mg/mL (n=1) which was then diluted 10 fold in 0.1 N hydrochloric acid and methanol (1:1 v/v) to give a 1 mg/mL solution. The concentration of test compound in the filtrate was quantified relative to the concentration standard.

Analysis was performed using a gradient HPLC-UV system with a total cycle time of 6 min. The UV detection was performed using a photodiode array detector acquired between 220 nm and 300 nm and total response was monitored.

Plasma Stability. The plasma of the relevant species was adjusted to pH 7.4 using either hydrochloric acid or sodium hydroxide depending on the initial pH of the plasma. Incubations were performed at a compound concentration of 1 μM in plasma, pH 7.4, at 37°C. The final DMSO concentration in the incubation was 2.5 %. Reactions were terminated following 0, 15, 30, 60 and 120 min by methanol containing internal standard. The sampling plate was centrifuged (2500 rpm, 45 min, 4 °C) and the supernatants from each time point pooled in cassettes of up to 4 compounds. Samples were analyzed for parent compound by LC-MS/MS using Cyprotex generic analytical conditions. The percentage of parent compound remaining at each time point relative to the 0 min sample was then calculated from LC-MS/MS peak area ratios (compound peak area/internal standard peak area).

Plasma Protein Binding (10%). Solutions of compound (5 μM, 0.5 % final DMSO concentration) were prepared in buffer (pH 7.4) and 10 % plasma (*v/v* in buffer). The experiment was performed using equilibrium dialysis with the two compartments separated by a semi-permeable membrane. The buffer solution was added to one side of the membrane and the plasma solution to the other side. Standards were prepared in plasma and buffer and incubated at 37 °C. Corresponding solutions for each compound were analyzed in cassettes by LC-MS/MS. After equilibration, samples were taken from both sides of the membrane. The solutions for each batch of compounds were combined into two groups (plasma-free and plasma-containing) then cassette analyzed by LC-MS/MS using two sets of calibration standards for plasma-free (7 points) and plasma-containing solutions (6 points). Cyprotex generic LC-MS/MS conditions were used. Samples were quantified using standard curves prepared in the equivalent matrix. The compounds were tested in duplicate.

Microsomal Stability. Pooled human liver microsomes (pooled male and female) and pooled mouse liver microsomes (male CD mice) were prepared at Cyprotex or were purchased from a reputable commercial supplier. Microsomes were stored at -80 °C prior to use. Microsomes (final protein concentration 0.5 mg/mL), 0.1 M phosphate buffer pH 7.4 and compound (final substrate concentration = 3 μM; final DMSO concentration = 0.25%) were pre-incubated at 37 °C prior to the addition of NADPH (final concentration = 1mM) to initiate the reaction. The final incubation volume was 25 μL. All incubations were performed singularly for each test compound. Each compound was incubated for 0, 5, 15, 30 and 45 min. The control (minus NADPH) was incubated for 45 min only. The reactions were stopped by the addition of 50 μL methanol containing internal standard at the appropriate time points. The incubation plates were centrifuged at 2,500 rpm for 20 min at 4 °C to precipitate the protein. Following protein precipitation, the sample supernatants were combined in cassettes of up to 4 compounds and analyzed using Cyprotex generic LC-MS/MS conditions.

Bi-directional Caco-2 Permeability. Caco-2 cells obtained from the ATCC were used between passage numbers 40-60. Cells were seeded on to Millipore Multiscreen Caco-2 plates at 1 x 10^5 cells cm^{-2}. They were cultured for 20 days in DMEM and media was changed every two or three

days. On day 20 the permeability study was performed. Hanks Balanced Salt Solution (HBSS) pH 7.4 buffer with 25 mM HEPES and 4.45 mM glucose at 37 °C was used as the medium in the permeability studies. Incubations were carried out in an atmosphere of 5 % CO2 with a relative humidity of 95 % at 37 °C.

On day 20, the monolayers were prepared by rinsing both basolateral and apical surfaces twice with HBSS at 37 °C. Cells were then incubated with HBSS in both apical and basolateral compartments for 40 min to stabilize physiological parameters. HBSS was then removed from the apical compartment and replaced with test compound dosing solutions. The solutions were made by diluting 10 mM compound in DMSO with HBSS to give a final test compound concentration of 10 μM (final DMSO concentration 1 %). The fluorescent integrity marker lucifer yellow was also included in the dosing solution. Analytical standards were made from dosing solutions. The apical compartment inserts were then placed into 'companion' plates containing fresh HBSS. For basolateral to apical (B-A) permeability determination the experiment was initiated by replacing buffer in the inserts then placing them in companion plates containing dosing solutions. At 120 min the companion plate was removed and apical and basolateral samples diluted for analysis by LC-MS/MS. Compound permeability was assessed in duplicate. On each plate compounds of known permeability characteristics were run as controls. Test and control compounds were quantified by LC-MS/MS cassette analysis using a 5-point calibration with appropriate dilution of the samples. Cyprotex generic analytical conditions were used. The starting concentration (C0) was determined from the dosing solution and experimental recovery calculated from C0 and both apical and basolateral compartment concentrations.

The integrity of the monolayers throughout the experiment was checked by monitoring lucifer yellow permeation using fluorimetric analysis. Lucifer yellow permeation was low if monolayers had not been damaged. If a lucifer yellow P_{app} value was above QC limits in one individual test compound well, then an n=1 result was reported. If lucifer yellow P_{app} values were above QC limits in both replicate wells for a test compound, the compound was re-tested. If on repeat, high lucifer yellow permeation was observed in both wells then toxicity or inherent fluorescence of the test compound was assumed. No further experiments were performed in this instance.

Supplementary References

1. Goncalves V, Brannigan JA, Thinon E, Olaleye TO, Serwa R, Lanzarone S*, et al.* A fluorescence-based assay for *N*-myristoyltransferase activity. *Anal Biochem* 2012, **421**(1)**:** 342-344.

2. Heal WP, Wright MH, Thinon E, Tate EW. Multifunctional protein labeling via enzymatic N-terminal tagging and elaboration by click chemistry. *Nat Protoc* 2012, **7**(1)**:** 105-117.

3. Gilson PR, Nebl T, Vukcevic D, Moritz RL, Sargeant T, Speed TP*, et al.* Identification and stoichiometry of glycosylphosphatidylinositol-anchored membrane proteins of the human malaria parasite *Plasmodium falciparum*. *Mol Cell Proteomics* 2006, **5**(7)**:** 1286-1299.

4. Srinivasan R, Tan LP, Wu H, Yang PY, Kalesh KA, Yao SQ. High-throughput synthesis of azide libraries suitable for direct "click" chemistry and in situ screening. *Org Biomol Chem* 2009, **7**(9)**:** 1821-1828.

5. Frearson JA, Brand S, McElroy SP, Cleghorn LA, Smid O, Stojanovski L*, et al. N*-myristoyltransferase inhibitors as new leads to treat sleeping sickness. *Nature* 2010, **464**(7289)**:** 728-732.

6. Brand S, Cleghorn LA, McElroy SP, Robinson DA, Smith VC, Hallyburton I*, et al.* Discovery of a novel class of orally active trypanocidal *N*-myristoyltransferase inhibitors. *J Med Chem* 2011, **55**(1)**:** 140-152.

7. Santos I, Paulo R, inventors; WO2008061792 (A2). 2008.

8. Badescu V, Camp A, Clack B, Cohen M, Filla S, Gallagher P*, et al.*, inventors; WO2008141020 (A1). 2008.

9. Goncalves V, Brannigan JA, Whalley D, Ansell KH, Saxty B, Holder AA*, et al.* Discovery of *Plasmodium vivax N*-myristoyltransferase inhibitors: screening, synthesis, and structural characterization of their binding mode. *J Med Chem* 2012, **55**(7)**:** 3578-3582.

10. Kabsch W. Xds. *Acta Crystallogr D Biol Crystallogr* 2010, **66**(Pt 2)**:** 125-132.

11. Evans P. Scaling and assessment of data quality. *Acta Crystallogr D Biol Crystallogr* 2006, **62**(Pt 1)**:** 72-82.

12. Winter G. xia2: an expert system for macromolecular crystallography data reduction. *J Appl Crystallogr* 2010, **43**(1)**:** 186-190.

13. Murshudov GN, Vagin AA, Dodson EJ. Refinement of macromolecular structures by the maximum-likelihood method. *Acta Crystallogr D Biol Crystallogr* 1997, **53**(Pt 3)**:** 240-255.

14. Emsley P, Lohkamp B, Scott WG, Cowtan K. Features and development of Coot. *Acta Crystallogr D Biol Crystallogr* 2010, **66**(Pt 4)**:** 486-501.

15. Ribaut C, Berry A, Chevalley S, Reybier K, Morlais I, Parzy D*, et al.* Concentration and purification by magnetic separation of the erythrocytic stages of all human *Plasmodium* species. *Malar J* 2008, **7:** 45.

16. Lambros C, Vanderberg JP. Synchronization of *Plasmodium falciparum* erythrocytic stages in culture. *J Parasitol* 1979, **65**(3)**:** 418-420.

17. Rees-Channer RR, Martin SR, Green JL, Bowyer PW, Grainger M, Molloy JE*, et al.* Dual acylation of the 45 kDa gliding-associated protein (GAP45) in *Plasmodium falciparum* merozoites. *Mol Biochem Parasitol* 2006, **149**(1)**:** 113-116.

18. Green JL, Rees-Channer RR, Howell SA, Martin SR, Knuepfer E, Taylor HM*, et al.* The motor complex of *Plasmodium falciparum*: phosphorylation by a calcium-dependent protein kinase. *J Biol Chem* 2008, **283**(45)**:** 30980-30989.

19. Uthaipibull C, Aufiero B, Syed SE, Hansen B, Guevara Patino JA, Angov E*, et al.* Inhibitory and blocking monoclonal antibody epitopes on merozoite surface protein 1 of the malaria parasite *Plasmodium falciparum*. *J Mol Biol* 2001, **307**(5)**:** 1381-1394.

20. Green JL, Martin SR, Fielden J, Ksagoni A, Grainger M, Yim Lim BY*, et al.* The MTIP-myosin A complex in blood stage malaria parasites. *J Mol Biol* 2006, **355**(5)**:** 933-941.

21. Olsen JV, de Godoy LM, Li G, Macek B, Mortensen P, Pesch R*, et al.* Parts per million mass accuracy on an Orbitrap mass spectrometer via lock mass injection into a C-trap. *Mol Cell Proteomics* 2005, **4**(12)**:** 2010-2021.

22. Perkins DN, Pappin DJ, Creasy DM, Cottrell JS. Probability-based protein identification by searching sequence databases using mass spectrometry data. *Electrophoresis* 1999, **20**(18)**:** 3551-3567.

23. Reorganizing the protein space at the Universal Protein Resource (UniProt). *Nucleic Acids Res*, **40**(Database issue)**:** D71-75.

24. Searle BC. Scaffold: a bioinformatic tool for validating MS/MS-based proteomic studies. *Proteomics*, **10**(6)**:** 1265-1269.

25. Craig R, Beavis RC. TANDEM: matching proteins with tandem mass spectra. *Bioinformatics* 2004, **20**(9)**:** 1466-1467.

26. Keller A, Nesvizhskii AI, Kolker E, Aebersold R. Empirical statistical model to estimate the accuracy of peptide identifications made by MS/MS and database search. *Anal Chem* 2002, **74**(20)**:** 5383-5392.

27. Nesvizhskii AI, Keller A, Kolker E, Aebersold R. A statistical model for identifying proteins by tandem mass spectrometry. *Anal Chem* 2003, **75**(17)**:** 4646-4658.

28. Pierleoni A, Martelli PL, Casadio R. PredGPI: a GPI-anchor predictor. *BMC Bioinformatics* 2008, **9:** 392.

29. Wisniewski JR, Zougman A, Nagaraj N, Mann M. Universal sample preparation method for proteome analysis. *Nat Methods* 2009, **6**(5)**:** 359-362.

30. Cheng Y-C, Prusoff WH. Relationship between the inhibition constant (KI) and the concentration of inhibitor which causes 50 per cent inhibition (I50) of an enzymatic reaction. *Biochem Pharmacol* 1973, **22**(23)**:** 3099-3108.

31. Janse CJ, Franke-Fayard B, Mair GR, Ramesar J, Thiel C, Engelmann S*, et al.* High efficiency transfection of *Plasmodium berghei* facilitates novel selection procedures. *Mol Biochem Parasitol* 2006, **145**(1)**:** 60-70.